PHILOSOPHICAL TRANSACTIONS OF THE ROYAL SOCIETY B BIOLOGICAL SCIENCES

The Topology of Cleavage Patterns with Examples from Embryos of Nereis, Styela and Xenopus

Valerie B. Morris, K. E. Dixon and R. Cowan

Phil. Trans. R. Soc. Lond. B 1989 **325**, 1-36
doi: 10.1098/rstb.1989.0072

Phil. Trans. R. Soc. Lond. B **325**, 1–36 (1989)

Printed in Great Britain

THE TOPOLOGY OF CLEAVAGE PATTERNS WITH EXAMPLES FROM EMBRYOS OF *NEREIS*, *STYELA* AND *XENOPUS*

BY VALERIE B. MORRIS,[1] K. E. DIXON[2] AND R. COWAN[3]

[1] *School of Biological Sciences, Zoology Building A*08, *University of Sydney, New South Wales* 2006, *Australia*

[2] *School of Biological Sciences, The Flinders University of South Australia, Bedford Park, South Australia* 5042, *Australia*

[3] *CSIRO Division of Mathematics and Statistics, Box* 218, *Lindfield, New South Wales* 2070, *Australia*

(*Communicated by D. T. Anderson, F.R.S. – Received* 3 *October* 1988)

CONTENTS

A theoretical scheme of cleavage is defined and used to construct topological maps of the cleavage patterns in embryos of *Nereis*, *Styela* and *Xenopus*. The maps are a projection of the surface of the embryo showing every blastomere and every neighbour of each blastomere. They simplify the cleavage pattern. The cellular arrangements observed in blastulae can be reconstructed from the topological maps after specifying the mechanics that shape cellular arrangements. The mechanics of

 [Published 31 August 1989

the rotations of blastomeres in the spiral cleavage of *Nereis* are found by these means. The maps of *Nereis* and *Styela* show the differences between spiral and bilateral cleavage. The map of *Xenopus* has bilateral symmetry and strongly resembles that of *Styela*. The variable cleavage patterns in *Xenopus* were recorded easily in topological maps. A numbering system for blastomeres of *Xenopus*, based on Conklin's scheme for *Styela*, is described for experimental use.

To explain the forms of cleavage patterns, we consider ways of dividing the plane into polygons each with six neighbours by lines drawn sequentially. Some ways have bilateral symmetry. We show how such partitioning of the plane can be transferred to a sphere. This allows cleavage patterns, which are a partitioning of a sphere, to be transferred back to the plane and so be compared with the partitioning that gives six neighbours. We conclude that cleavage patterns have features that bias the number of neighbours of each cell towards six.

The forms of cleavage patterns, it is suggested, preserve spatial information in the cytoplasm, such as that set up during oogenesis and during ooplasmic segregation after fertilization, during the partitioning of the zygote into cells. They could be mechanically stable ways of dividing the zygotic cytoplasm that reduce stresses so blastomeres do not shift and disrupt the established spatial values. The apparently conflicting views of Thompson (*On growth and form*. Cambridge University Press (1917)), who believed cleavage patterns were determined solely by mechanical forces, and Wilson (*The cell in development and heredity*. New York: Macmillan (1925)), who argued that cleavage patterns had promorphological significance, may thus be reconciled.

1. Introduction

Cleavage is the division of a single-celled zygote into a many-celled blastula. Much of current knowledge of the pattern of the divisions is based on studies done last century and early this century (see Wilson 1925). The kinds of cleavage patterns named and described then and still referred to in textbooks of developmental biology (see, for example, Berrill & Karp 1976) are spiral, bilateral and radial. The common view is that spiral cleavage is the form found in polychaetes, molluscs (excepting cephalopods), nemerteans and turbellarians, bilateral cleavage is typical of ascidians and radial cleavage is typical of echinoderms.

A new and simplifying way of describing cleavage patterns is reported here, one that makes it easy to see the similarities and differences between cleavage patterns in individuals of one species and between those in widely different animal groups. The method was devised to handle the variable cleavage patterns in *Xenopus laevis* (Amphibia) in experimental work, but when it was tested on some classical descriptions of cleavage (Wilson 1892; Conklin 1905) we found it gave insight into cleavage generally. The method enabled us, for example, to identify the sources of rotation in spiral cleavage. More importantly, similarities in the cleavage patterns of *Xenopus* and *Styela partita* (Stimpson) (Ascidiacea), as described by Conklin (1905), became clear and we have constructed a nomenclature for the blastomeres of *Xenopus*, modified only slightly from that used by Conklin for *Styela*; the nomenclature has practical experimental value.

The role of a conserved cleavage pattern in development is still not understood. In a classic account, Wilson (1925) argued that the patterns had promorphological significance and were not determined simply by mechanical forces as Thompson (1917) had suggested. Here, we resolve these two views by suggesting that cleavage patterns are a mechanically stable form of partitioning that reduces any tendency of cells to re-position after a division. The zygotic cytoplasm is divided during cleavage into cells separated by plasma membranes but these

PHILOSOPHICAL TRANSACTIONS OF THE ROYAL SOCIETY B BIOLOGICAL SCIENCES

membranes adhere to each other as each division is completed (Ohshima & Kubota 1985). If cleavage is not mechanically stable, shearing forces might cause the membrane faces to slip past one another. This would disarrange any cytoplasmic spatial field set up during oogenesis and that set up during the first cleavage cycle after sperm entry (Conklin 1905; Gerhart *et al.* 1984) and disturb what might otherwise appear as promorphological values carried in cell lineages.

We arrived at these views through a topological analysis of the classical descriptions of cleavage in *Nereis limbata* Ehlers (Polychaeta) (Wilson 1892) and *Styela* (Conklin 1905) and a similar analysis of our observations of cleavage in *Xenopus*. The analysed patterns are compared with the sequential partitioning of planar space that leads to polygons, each with six neighbours, after every partitioning cycle. We find that cleavage patterns have features that bias the number of neighbours about a cell towards six. Such hexagonal cellular arrangements are regarded as a natural and stable configuration (Thompson 1917).

2. Descriptions of cleavage patterns

An embryo that is undergoing cleavage is a somewhat complex arrangement of cells. To simplify this arrangement, we draw a topological map of the cleavage pattern based on the general scheme described below.

(*a*) *The general scheme of cleavage*

The partitioning is described first for a sphere. In figure 1, a sphere is partitioned first into hemispheres, then into quadrants and then into octants by three orthogonal primary planes. After this, each octant is partitioned by a fourth plane which is orthogonal to the third primary plane and parallel to either the first or second primary planes. Fifth planes are orthogonal to fourth planes and so are parallel to either of two primary planes (figure 1). The primary planes to which fourth and fifth planes are parallel can vary between octants. Further partitioning is alternately parallel first to fourth planes and then to fifth planes. So, partitioning in each octant is a series of orthogonal planes limited in orientation to being parallel to only two primary planes. Each new set of planes always intersects the set of last-formed planes as well as some formed earlier.

In an embryo, the partitioning is into cells (blastomeres) and because each blastomere divides separately, the actual division planes are now grouped appropriately into those of the first, second, third, and so on, cleavage cycles. For simplicity, we draw the plane dividing each blastomere as a line on the outer surface of the embryo. Importantly, the division lines of the same cleavage cycle do not now meet lines of previous cycles at four-radiate junctions, as in figure 1. They are offset creating a pair of three-radiate junctions (figure 2*a*). We call the line segment between the pair of three-radiate junctions an *offset*. The orthogonal framework of figure 1 now acts to unify the separate and offset division lines of each cleavage cycle. The orthogonal succession of division lines is discussed further in §3.

Thus the cleavage of an embryo is represented by sets of division lines, one set for each cleavage cycle, with lines of the same cycle in adjacent blastomeres meeting the line of a previous cycle and creating an offset. To draw a cleavage pattern, it is convenient to project the surface of the embryo as quadrants in the plane. The lines of the first and second cleavage cycles become the boundaries of the quadrants. The sets of lines of the third and subsequent cleavage cycles are then drawn on the quadrants. Examples of such topological maps are shown in figure 3.

PHILOSOPHICAL TRANSACTIONS OF THE ROYAL SOCIETY B BIOLOGICAL SCIENCES

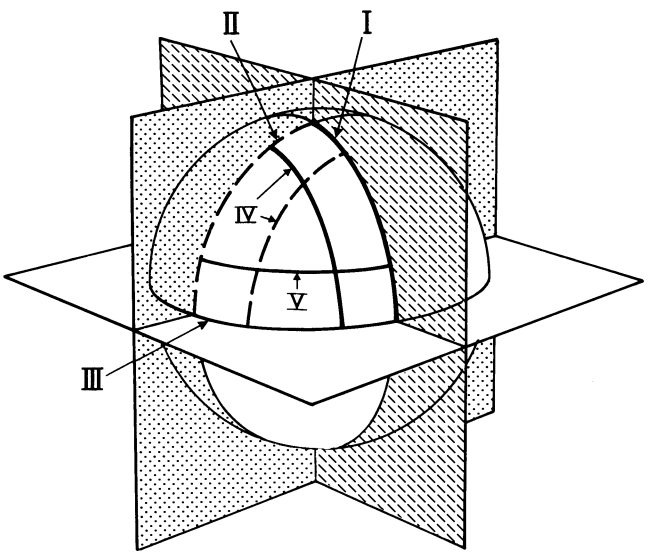

FIGURE 1. The partitioning of a sphere. Three primary planes I, II, and III divide the sphere successively into hemispheres, quadrants and octants. Each octant is then divided by a fourth plane (IV) which can be parallel to I or II; the two possible positions are drawn as surface lines on one octant. A fifth plane is orthogonal to a fourth plane and so occupies a position parallel to III (surface line labelled V) or the vacant position after a fourth plane is set. If the fourth plane is parallel to I and the fifth is parallel to II, a three-sided face is attached to III; if fourth and fifth planes are parallel to I and III respectively, a three-sided face is attached to II; these three-sided faces are examples of the residual polygons referred to later in the text.

Successive sets of lines are only notionally orthogonal, as they cannot be represented as such in the plane. Also, lines of the fourth and later cycles are only notionally parallel to the primary lines. The primary line to which a line of the fourth cycle is parallel, for example, is defined by the two primary lines it intersects; it is parallel to the first line if it intersects the second and third lines, as implied above in the partitioning of the sphere.

We name two types of offsets in the topological maps. The first is the M offset created where division lines in two sister cells meet the line in their mother cell (figure 2*b*); this will always occur where division lines of the current cycle are orthogonal to those of the previous cycle. The second is the C offset. It is the offset created by the other end of a division line, away from the M offset, where it and another line of the current cycle in the adjacent cell meet the line of a cleavage cycle earlier than the last (figure 2*b*).

Using this scheme, we draw topological maps of cleavage in *Nereis*, *Styela* and *Xenopus* up to the fifth or sixth cleavage cycle. The method is especially useful for recording a variable cleavage pattern, such as occurs in *Xenopus*. The cleavage pattern is simplified because each cycle of cleavage divisions is drawn as a set of lines that do not distort those of the previous cycle, as they would in life.

We have not used the option of magnitude available in the scheme because our interest here is in the topology of cleavage patterns. Magnitudes of membrane lengths and angles of intersection would, of course, give a precise description of the patterns. Such measurements would be needed to compute the mechanical forces governing the arrangements of cells in an embryo and explore the degree of mechanical stability.

PHILOSOPHICAL TRANSACTIONS OF THE ROYAL SOCIETY B BIOLOGICAL SCIENCES

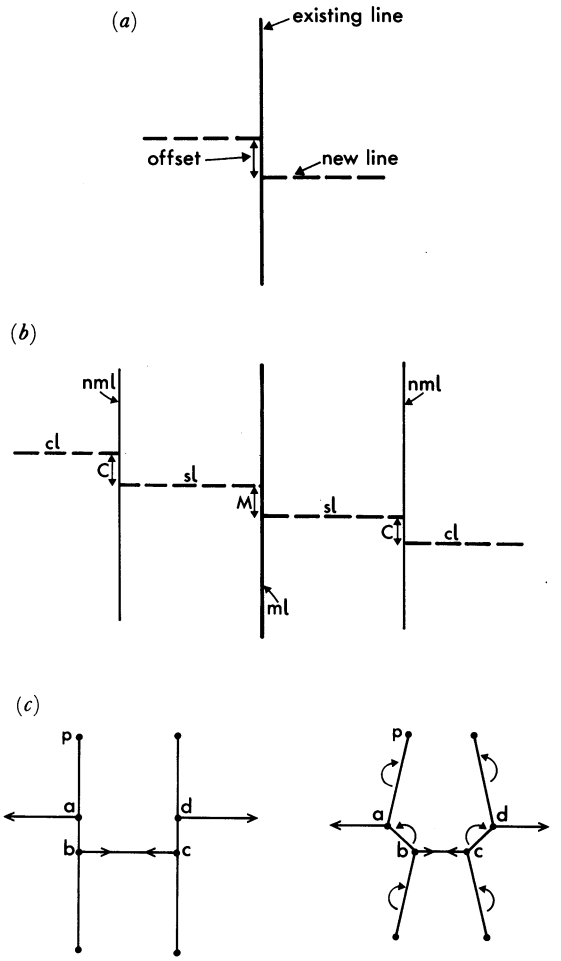

FIGURE 2. Offsets and turning couples. (*a*) The offset is the line segment between the points on an existing line where two new division lines in adjacent cells meet it, each making a three-radiate junction. (*b*) M and C offsets. An M offset (M) is formed on the division line (ml) in a mother-cell by division lines (sl) in two sister cells contacting ml at separate points. A C offset (C) is formed on a non-mother-cell line (nml) by the other end of sl and a division line (cl) of the same cleavage cycle in a cell of some cousin-relationship contacting nml at separate points. (*c*) Turning couples at offsets. Opposite forces applied at a and b create a sinistral couple and turn the offset ab sinistrally; opposite forces applied at c and d create a dextral couple and turn the offset cd dextrally. The force applied at a also creates a dextral couple about pivot point p, turning the external line ap dextrally; similarly, the external line acted on by the force at b is turned dextrally; the external lines acted on at c and d are turned sinistrally. The displacement of offsets and external lines is shown on the right with curved arrows indicating the directions of turning couples.

(i) *The mechanics at offsets*

Before describing the topological maps, we show the mechanics operating at offsets due to the contraction forces generated during cytokinesis. Knowing these mechanics, we can recreate the arrangements of blastomeres from the topological maps.

In an embryo, each cleavage furrow, which appears at the start of cytokinesis, contracts and applies forces to the existing boundaries between blastomeres. We represent this for two adjacent cells as opposite forces applied to an existing line by two new division lines; the forces are applied at the ends of the offset, creating a turning couple (figure 2*c*). The sense of the couple can be clockwise (dextral) or anticlockwise (sinistral). The turning couple displaces the

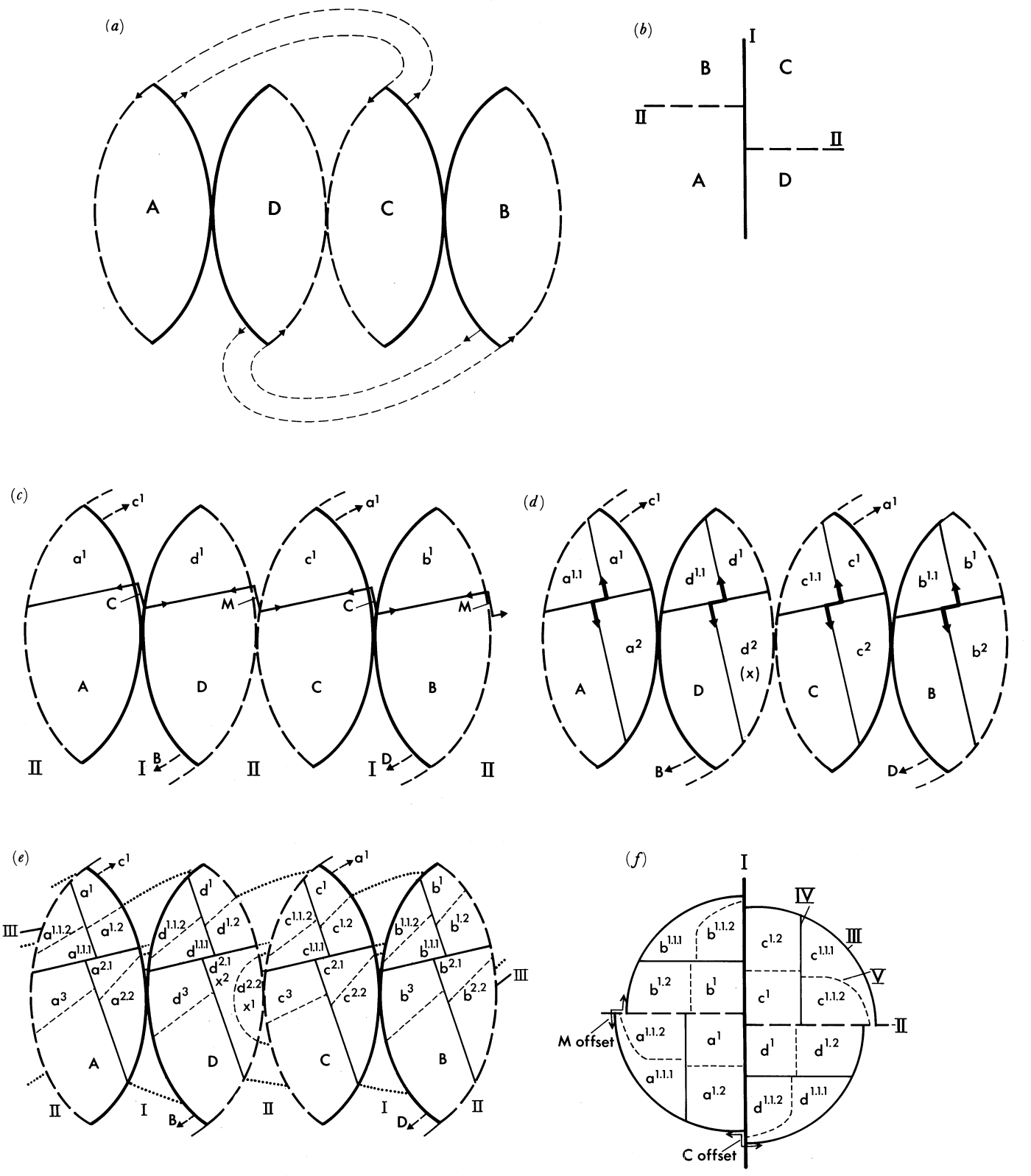

FIGURE 3. For description see opposite.

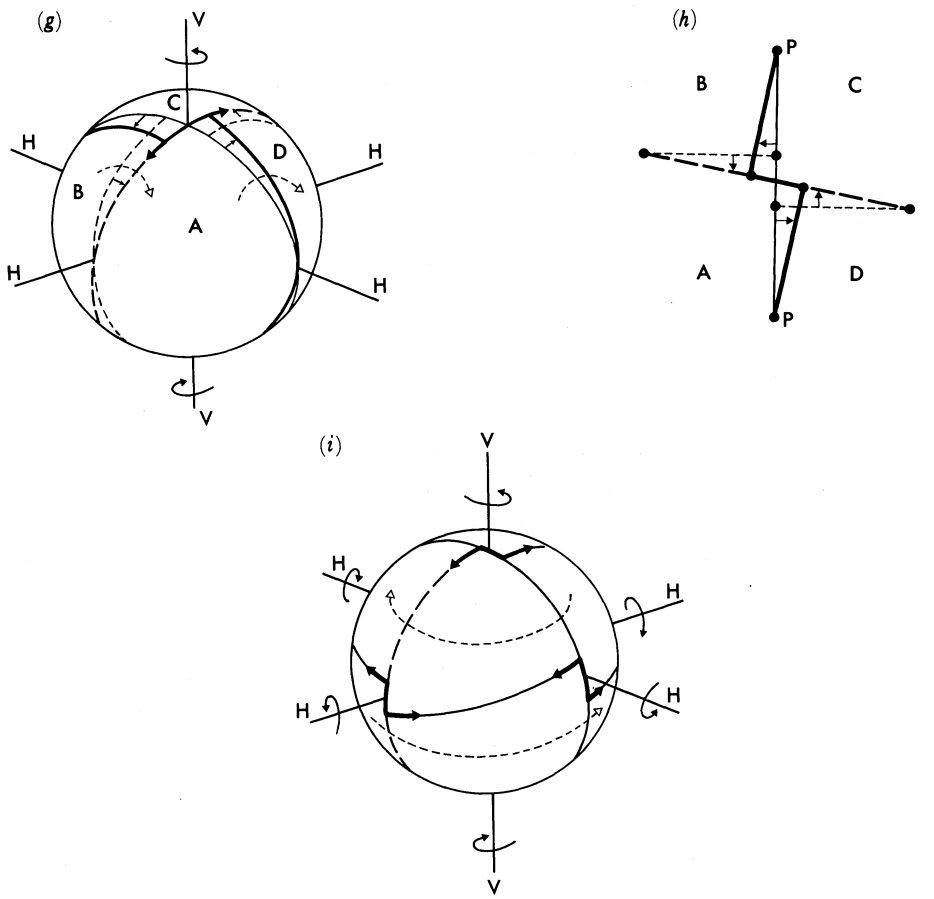

FIGURE 3. Cleavage in *Nereis*. (*a*) The quadrants, A, D, C and B formed at the second cleavage cycle. The M offsets (polar offsets) are created by second lines that are extended as pairs of dashed lines to indicate the same offset; the couple is sinistral at both offsets (arrows). Animal pole is uppermost here and in (*c*), (*d*) and (*e*). (*b*) The M offset at the animal pole in polar view. A and C are in contact along the polar offset. (*c*) The third cleavage cycle. The M offsets (M) made by third lines are on the second lines and the C offsets (C) are on the first line. Third lines are tilted anticlockwise from the horizontal and all couples are sinistral. (*d*) The fourth cleavage cycle. The M offsets made by fourth lines (heavy arrows) are on the third lines and all couples are sinistral. Fourth lines if parallel to the first in an animal octant are parallel to a second line in the sister vegetal octant, for example, the fourth line in the a^1-octant (see (*c*)) is parallel to the first line but in the A-octant it is parallel to a second line; similarly for the c^1-octant and the C-octant; in d^1 and b^1, fourth lines are parallel to a second line and in D and B they are parallel to the first line. The d^2 blastomere in *Nereis* is named X. (*e*) The fifth cleavage cycle. The M offsets made by fifth lines are on fourth lines and the couples are sinistral. The orientations of fifth lines are parallel to third lines except in the division of blastomere X. The C offsets made by fifth lines in a^2 and $d^{1.1}$, c^2 and $b^{1.1}$, and b^2 and $a^{1.1}$ are sinistral and form anomalously within the M and C offsets of the third cleavage cycle; mixed-cycle couples are formed by other fifth lines and fourth lines. (*f*) The fifth cleavage cycle in the animal hemisphere in polar view. Orientations of fourth lines alternate from parallel to the first (a and c octants) and parallel to the second (b and d octants). Fifth lines are parallel to third lines. (*g*) Effects of turning couples at the second cleavage cycle in *Nereis*. The sinistral couple at the animal polar offset (uppermost) turns the offset sinistrally, opposing a sinistral turn of the vegetal polar offset (not visible in the figure) and leads to a dextral twist of the A+D and C+B blastomeres about their respective end of a horizontal axis (H); B+A and D+C blastomeres are twisted similarly; dashed arrows indicate the twists in A+D and B+A; light lines show the positions of cleavage lines before the twists occur and heavy lines show positions after twisting; curved arrows show the twists about the vertical axis (V). (*h*) Effects of the turning couple at the animal polar offset. The polar offset is turned sinistrally; external lines are turned dextrally about pivot points p; the contracting lines are themselves also turned dextrally about other pivot points. The positions of cleavage lines are shown before (light lines) and after (heavy lines) the couple takes effect. (*i*) Effects of turning couples at the third cleavage cycle in *Nereis*. Sinistral couples at the M and C offsets (heavy arrows) of the third cleavage cycle turn each offset sinistrally about a horizontal axis (H), driving an upper tier of octants dextrally about the animal pole (uppermost) and a lower tier dextrally about the vegetal pole when viewed from the respective pole; dashed arrows show the direction of rotation in each tier. The positions of cleavage lines are those before displacement. The naming of blastomeres in this and other figures of *Nereis* is according to Wilson (1892).

PHILOSOPHICAL TRANSACTIONS OF THE ROYAL SOCIETY B BIOLOGICAL SCIENCES

existing cleavage line. In a dextral couple, the offset itself is turned clockwise (dextrally) and in a sinistral couple, it is turned anticlockwise (sinistrally) (figure 2*c*). The existing line either end of the offset, named an external line, is also displaced. Each external line is turned about a pivot point distal from the offset in a couple of the opposite sense to that at the offset (figure 2*c*). The new division lines are also displaced (see below). These mechanics shape the arrangements of cells in an embryo. The arrangements can be considered simply as deformations of the existing boundaries between cells. We show later for *Nereis* the arrangements of cells recreated from the topological maps by allowing the turning couples at offsets to displace cleavage lines.

(*b*) *Application to Nereis*

We present first a topological map of cleavage in *Nereis*, using the description by Wilson (1892) and his notation. This is the classic account of spiral cleavage, in which Wilson named spiral cleavage as a type. From his detailed drawings we map cleavage up to the 32-cell stage.

The first cleavage line (first line) divides the zygote into the AB and CD blastomeres. The second cleavage lines (second lines) divide the A from the B blastomere and the C from the D blastomere; these are the quadrants of the scheme (figure 3*a*). The offset at the animal pole made where the second lines meet the first line is the polar furrow (offset) along which blastomeres A and C are in contact (figure 3*b*). At the vegetal pole, blastomeres B and D are in contact along a vegetal polar offset. Strictly speaking, both these offsets are M offsets because they are formed by cleavage lines in sister cells meeting the line in their mother-cell; both couples are sinistral. At the third cleavage cycle (figure 3*c*), there are M offsets where third cleavage lines (third lines) meet second lines and C offsets where third lines meet the first line; all the couples are sinistral. The fourth cleavage lines (fourth lines) (figure 3*d*) are between a third line and either a second line or the first line. Those that form in the octants a^1, c^1, D and B (figure 3*c*) are from the third line to a second line and so are parallel to the first line (figure 3*d*). Those in the octants d^1, b^1, A and C are from the third line to the first line and so are parallel to the second lines. The orientation of a fourth line alternates in polar view from parallel to the first line, then parallel to the second, beginning say at octant a^1 in the animal hemisphere or octant D in the vegetal hemisphere (figure 3*c*, *d*, *f*). The M offsets formed by fourth lines are on the third lines (figure 3*d*); the couples are again sinistral. There are no C offsets, because the orientations of fourth lines alternate, as just described (figure 3*f*). The orientations of fifth cleavage lines (fifth lines) (figure 3*e*) are defined by the contacts made by the ends of the pair of lines in each octant, that is, the ends away from the M offset. In all except the D vegetal octant, one end of the pair is on a first line and the other is on a second line so the pair is parallel to the third line (figure 3*e*, *f*). The M offsets are on fourth lines and the couples are sinistral, except again in the vegetal D octant. There are now C offsets made by the fifth lines in a^2 and $d^{1.1}$, c^2 and $b^{1.1}$, and b^2 and $a^{1.1}$; the couples are sinistral (figure 3*d*, *e*). The other fifth lines form mixed-cycle couples with the non-M-offset ends of fourth lines (figure 3*e*, *f*); these are sinistral in the animal octants but dextral in the vegetal octants. The fifth line in d^2 or X, the first somatoblast (Wilson 1892), cuts off blastomere x^1 to the right. There is no M offset in the vegetal D octant at the fifth cleavage cycle (figure 3*e*).

In these maps of *Nereis*, most cleavage lines of the same cleavage cycle meet at offsets, that is, they make pairs of three-radiate junctions on existing cleavage lines. The three-radiate pairs of the polar offsets are brought about by second lines tilted anticlockwise from a meridian. The three-radiate pairs of the third cleavage cycle are brought about by third lines each tilted

PHILOSOPHICAL TRANSACTIONS OF THE ROYAL SOCIETY B BIOLOGICAL SCIENCES

anticlockwise with respect to the equator (figure 3*c*). The fourth lines, notionally orthogonal to third lines, take orientations parallel to the first or second lines (figure 3*d*). The fifth lines, notionally orthogonal to fourth lines, take the orientation parallel to third lines, rather than to either the first or second lines. High-angle tilts of third lines allow some C offsets of the fifth cycle to form within the M and C offsets of the third cycle. The spiral type of cleavage depends on junctions having the three-radiate form.

The topological map in figure 3*e* shows both the animal and vegetal hemispheres and so similarities in the patterns between quadrants become clear, as well as the differences, for example, the special division of the first somatoblast. All M and C offsets in *Nereis* are sinistral, as are the mixed-cycle couples between the fourth and some fifth lines in the animal hemisphere.

(i) *Results of the topological analysis of Nereis*

Having now identified the offsets in *Nereis* and documented them in the topological maps, the turning couples can be allowed to act. We then find first how the rotations of blastomeres in spiral cleavage, noted classically, come about and then secondly derive the arrangements of blastomeres in *Nereis* from the maps. The forces generated at cytokinesis are imagined to contract the current division lines in our scheme and so shift the existing cleavage lines.

The actions of the turning couples. The actions of the turning couples are described at each successive cleavage cycle, remembering that the couples at all M and C offsets in figure 3 are sinistral. At the first cleavage cycle, no couple is generated because there is only one contracting line. At the second cleavage cycle, the two contracting second lines turn each polar offset sinistrally about the polar (vertical) axis, though no further than a point where the offset and the contracting lines are in line (figure 3*g*). Both offsets turn the same way when viewed from their respective pole. The external lines, which are here the two portions of the first line between the offsets, are turned dextrally about a horizontal axis by the contracting second lines (figure 3*g*). As the lines turn, the A+D and C+B blastomeres each rotate dextrally about a horizontal axis, as do less obviously the B+A and D+C blastomeres. In a polar view (figure 3*h*), the four blastomeres twist sinistrally about the pole. At the third cleavage cycle (figure 3*i*), the M offsets again turn sinistrally and the external lines turn dextrally, the latter about a pivot point at one end of the polar offset; the external lines are the portions of second lines between the M offsets and the polar offsets. The C offsets are also turned sinistrally and the external lines associated with them are also turned dextrally; the external lines here are the portions of the first line between the C offsets and polar offsets (figure 3*i*). The dextral turn of the external lines drives an upper tier of four animal blastomeres dextrally about the vertical axis. The rotation is of greatest magnitude next to the equator (figure 3*i*). The vegetal tier is similarly driven dextrally when viewed from the vegetal pole.

At the fourth cleavage cycle, the M offsets are on the just-established third lines. Sinistral couples again turn offsets sinistrally and external lines dextrally, this time within a quadrant (figure 3*d*). The sinistral turn of each offset adds another dextral displacement about the poles. The fourth lines do not form C offsets so each turns a segment of first or second line sinistrally about one end of a polar offset. There is thus a sinistral movement next to the poles contrasting with a dextral movement next to the equator. At the fifth cleavage cycle, an M offset is turned sinistrally in an octant (figure 3*e*). The C offsets, operating within the M and C offsets made at the third cleavage cycle, add again to the dextral displacement next to the equator. The

PHILOSOPHICAL TRANSACTIONS OF THE ROYAL SOCIETY B BIOLOGICAL SCIENCES

mixed-cycle, sinistral couples that fifth lines make with fourth lines in the animal hemisphere turn portions of the first or second lines between these quasi-offsets and the polar offsets, equivalent to external lines, dextrally about the poles.

In *Nereis* (figure 3*g*, *h*, *i*), the turning couple at an offset turns the offset sinistrally and both external lines dextrally. As well, the contracting lines are turned dextrally about distal pivot points, making a total of four lines turned dextrally by the couple (figure 3*h*). The relative movements of these four lines differ, however, and hence the relative movements of the blastomeres at the offset differ also. In figure 3*h*, the line between A and D pivots to the right whereas that between C and B pivots to the left, and so blastomeres A+D and C+B swing away from each other. At the same time, the line between B and A and that between D and C, originally set apart by the orientation of the offset, turn towards each other as the offset turns (figure 3*h*) so the B+A blastomeres and the D+C blastomeres swing towards each other. These relative displacements occur whenever pairs of contracting lines apply forces at an offset. In contrast, a single force acting on an existing line applies couples of the opposite sense to the line segments on either side of the point of applied force. We point out with respect to blastomere displacement that at the second cleavage cycle, the sinistral rotation about the vertical axis is accompanied by dextral rotations about two orthogonal horizontal axes (figure 3*g*). Similarly at the third cleavage cycle, the sinistral rotations of blastomeres about the M and C offsets, which have horizontal axes, are accompanied by a dextral rotation about the vertical axis. At later cleavage cycles, these coordinate orthogonal rotations are lost.

By identifying the actions at a turning couple, we can say how each offset, each external line and each contracting line will turn and thus how blastomeres will be arranged in an embryo. We can expect these events to occur whenever two newly forming division lines meet at an offset on a line formed at a previous cycle.

Arrangements of cells in polar view. To complete this account, we derive the actual arrangement of cells in *Nereis* from the topological maps. This is done for an animal-pole view up to the 32-cell stage (figures 4 and 5). The topological map of the third cleavage cycle (figure 4*a*) is first transformed by a sinistral turn of the polar offset and dextral turns of segments of the first and second lines to which the offset connects. It is then further transformed by sinistral turns of the M and C offsets of the third cleavage cycle and synergic dextral turns of the same segments of the first and second lines (figure 4*c*). The topological map of the fourth cleavage cycle (figure 4*b*) is transformed first to the arrangement in figure 4*c*. The fourth lines then contract and apply opposite couples to segments of the first and second lines turning the set connected to the polar offset sinistrally (figure 4*d*).

The topological map of the fifth cleavage cycle (figure 5*a*) is transformed first to the arrangement in figure 5*b* where fifth lines are drawn on the rearranged animal blastomeres of a 16-cell stage. The fifth lines contract and turn the M offsets sinistrally and the sets of four lines connected to them dextrally. Each group of four first cousins twists sinistrally in the region of the offset, as did the four first cousins in the region of the pole at the second cleavage cycle. The fifth lines between blastomeres 1 and 1.2 also apply a single force to segments of the first and second lines, pivoting a set connected to the polar offset dextrally; the polar quartet rotates dextrally.

Classical spiral cleavage. The classically named spiral cleavage refers to the alternate production of blastomeres, viewed laterally, to the left at odd-numbered cleavage cycles and to the right at even-numbered cycles, in a vegetal-to-animal direction (Wilson 1925). These

PHILOSOPHICAL TRANSACTIONS OF THE ROYAL SOCIETY B BIOLOGICAL SCIENCES

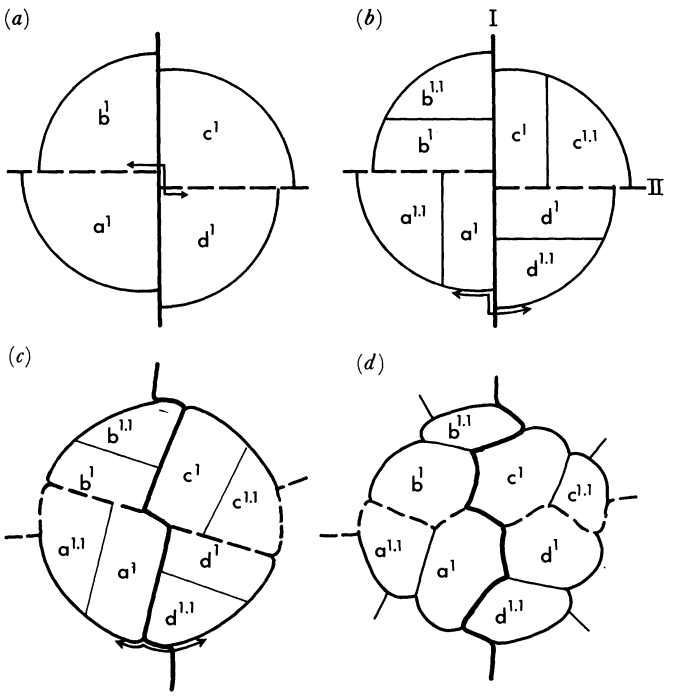

FIGURE 4. Cellular arrangements in *Nereis* derived from topological maps of (*a*) the first to third cleavage cycles and (*b*) the first to fourth cleavage cycles in the animal hemisphere. In (*c*) cleavage-line displacements are shown after the turning couples of the second and third cleavage cycles take effect but before the couples due to fourth lines, marked by a thin continuous line in each octant, do so. (*d*) Cellular arrangement after the couples of the fourth cleavage cycle act. The arrangement in (*d*) should be compared with figure 14 in Wilson (1892).

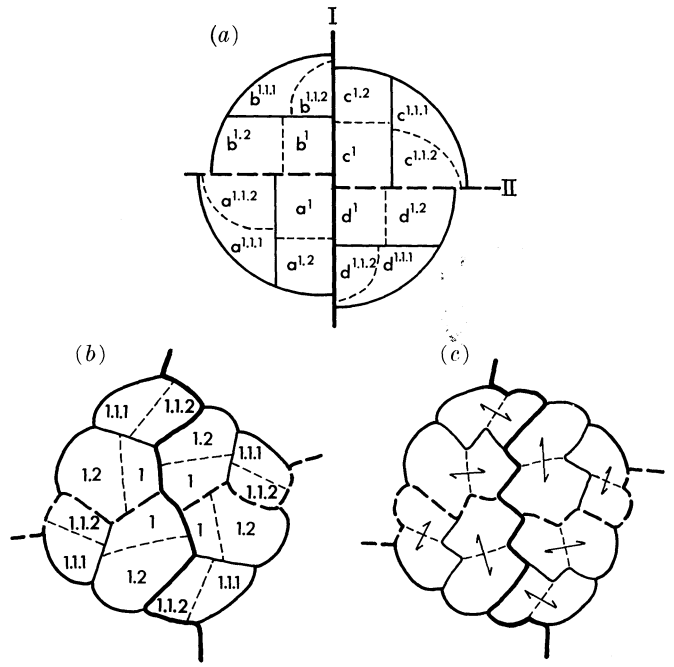

FIGURE 5. Cellular arrangements in *Nereis* derived from a topological map of (*a*) the 32-cell stage viewed from the animal pole. (*b*) Cleavage-line displacements after the fourth cleavage cycle but before the fifth cycle; fifth lines (thin dashed lines) are marked on cells of the 16-cell stage. (*c*) Cellular arrangement after the fifth cleavage cycle; half-arrows link sister cells. The arrangement in (*c*) should be compared with figure 23 in Wilson (1892).

PHILOSOPHICAL TRANSACTIONS OF THE ROYAL SOCIETY B BIOLOGICAL SCIENCES

same cleavage cycles viewed from the animal pole are described as dexiotropic (right-turning) and laeotropic (left-turning) alternately. Spiral cleavage is attributed to the inclination of the planes of division away from the strictly meridional and para-equatorial planes of orthoradial cleavage (Wilson 1925). Actual rotations of blastomeres were noted then as well. We show the rotations depend on the turning couples at offsets. Specifically, sinistral M and C offsets are required at the third cleavage cycle to produce a dextral rotation about either pole. The sense of the offset determines the direction of the rotation. We expect the sense of offsets in sinistral gastropods where the spiral direction is reversed (Wilson 1925) would be reversed also; for example, they would be dextral rather than sinistral at the third cleavage cycle. The cleavage lines in spiral cleavage meet at three-radiate junctions with angles settling to about 120° after the turning couples subside, in contrast to the four-radiate junctions featured in orthoradial cleavage, though Conklin (1897) considered the latter to be rare. Classical types of cleavage are commented on further in §4.

(*c*) *Application to Styela*

We draw next a topological map of *Styela* to show the features of bilateral cleavage. We indicate how it differs from spiral cleavage and, later, how the patterns in *Xenopus*, an amphibian, resemble the pattern in *Styela*, a protochordate. The topological map of cleavage in *Styela* is drawn from the classical description by Conklin (1905) whose notation we use. In the map (figure 6*a*), the A quadrants are anterior and the B quadrants are posterior; underlined letters indicate the right side of the embryo.

The first offsets, the polar offsets, which are M offsets formed at the second cleavage cycle, are short and in being so preserve an appearance of bilateral symmetry about the first cleavage line. The obvious bilateral symmetry, however, emerges at the third cleavage cycle. In both A and B on the right of the embryo (figure 6*a*), the third line is tilted anti-clockwise from the horizontal, as in *Nereis*, but in A and in B on the left the tilt is clockwise. These tilts were noted especially in the posterior blastomeres by Conklin and are clear in the well-known right-side view of *Styela* (figure 6*b*). The fourth lines (figure 6*a*), being orthogonal to third lines, are oriented symmetrically by the tilts of the third lines in the left and right quadrants. In the anterior animal octants, left and right, each fourth line is parallel to a second line. In the anterior vegetal octants, left and right, each fourth line is parallel to the first line. So, the fourth lines are inclined from second lines towards the first in a vegetal-to-animal direction in the anterior quadrants. In the posterior quadrants, the fourth lines are also inclined symmetrically on each side but each is parallel to a second line in the vegetal octants and parallel to the first line in the animal octants. These inclinations of fourth lines contribute to bilateral symmetry in the cleavage pattern. They are the source of the well-known symmetry of the 16-cell blastula viewed from the animal pole (figure 6*c*) or vegetal pole (figure 6*d*). These two polar views become similar if one is rotated through 180°.

The fifth lines (figure 6*a*) are classed as parallel to the third in all anterior octants because the ends of each pair contact the first and second lines. In the posterior vegetal octants, they are parallel to the first because these ends contact the third and second lines. In the posterior animal octants, the fifth line between blastomeres 6.5 and 6.6 is parallel to the first because it extends from a third to a second line; it does not intersect the mother-cell line. Between blastomeres 6.7 and 6.8, the orientation is ambiguous because there is only one contact on a primary line and so the line could be parallel to the second or third line.

The sixth cleavage lines (sixth lines) have a complex pattern (figure 6*a*). Often they do not

PHILOSOPHICAL TRANSACTIONS OF THE ROYAL SOCIETY B BIOLOGICAL SCIENCES

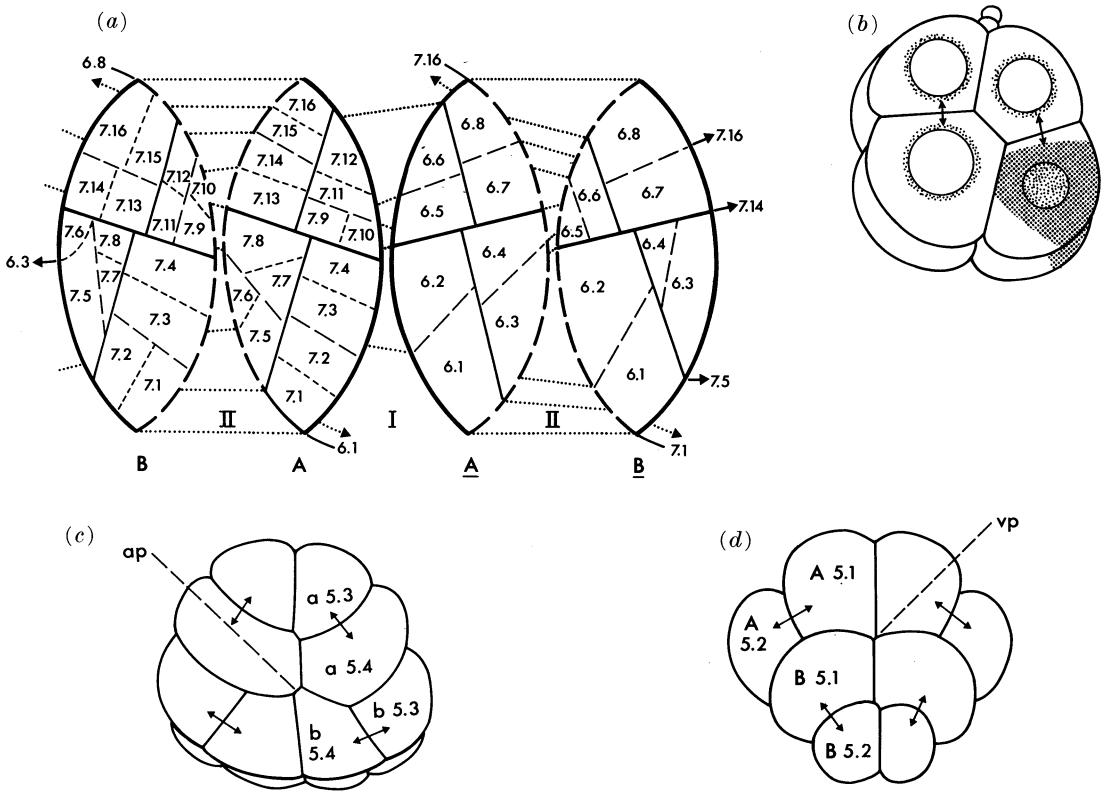

FIGURE 6. Cleavage in *Styela* (see text). (*a*) A topological map of the quadrants with animal pole uppermost. A and A, anterior quadrants; B and B, posterior quadrants; underlined letters are right side of embryo; blastomeres named by numbers only. Cleavage lines up to the fifth (thin dashed lines) shown in A and B; cleavage lines up to the sixth (short dashed lines) shown in B and A. Dotted lines between quadrants are continuations of cleavage lines to show the blastomere they contact. The numbering of blastomeres is according to Conklin (1905). (*b*) The well-known right-side view of cleavage in *Styela*, anterior to left, posterior to right, animal pole with polar bodies uppermost; double-headed arrows link sister cells; shaded region in posterior vegetal blastomeres is the yellow crescent; after figure 32 in Conklin (1905) where, for Conklin, the vegetal pole is dorsal. The characteristic arrangement of cells is caused by the prominent sinistral M offset formed at the third cleavage cycle (shown on the second line between A and B in (*a*)). (*c*) 16-cell stage viewed from animal pole (ap). (*d*) 16-cell stage viewed from vegetal pole (vp). The cellular arrangement in (*d*) is similar to that in (*c*) if (*d*) is rotated by 180°; after figures 38 and 37 in Conklin (1905).

intersect the mother-cell line. Those that form the anterior vegetal blastomeres 7.1, 7.2, 7.3 and 7.4 and the anterior animal blastomeres 7.11, 7.12, 7.13, 7.14, 7.15 and 7.16 are parallel to lines of the fifth cycle, rather than orthogonal to them. In posterior octants, the sixth lines that form the 7.3 and 7.4, and 7.5 and 7.6 cells, do not contact the mother-cell line; the rest do. The posterior 7.6 blastomeres are odd cells tucked against the first line; they remain undivided for several generations (Conklin 1905). The posterior blastomeres, 7.1 and 7.2, and the anterior blastomeres, 7.1, 7.2, 7.3 and 7.4, form a column of cells each side of the midline and contribute to chorda and neural plate. The 7.1 blastomeres about the vegetal pole are where invagination begins. Cleavage in *Styela* at this stage constructs a particular arrangement of cells.

So in *Styela*, and in *Nereis*, current cleavage lines form pairs of three-radiate junctions and hence offsets on existing lines where an orthogonal succession is followed. The three-radiate pairs again depend on tilted cleavage lines. But in *Styela*, the third lines are tilted clockwise from

the horizontal on the left and anti-clockwise on the right, making the M offset on the left dextral and that on the right sinistral (figure 6*a*). It is these tilts and offsets that give bilateral symmetry to the cleavage pattern in *Styela*. The symmetrical orientations of fourth lines follow from them. In *Nereis*, all third lines are tilted anti-clockwise from the horizontal making all the offsets of the third cycle sinistral (figure 3*c*). In *Nereis*, these sinistral offsets lead to a rotation of a tier of blastomeres dextrally about each pole. In *Styela*, the M offsets at the third cycle are of opposite sense and the turning couples there produce opposing rotations. The two animal octants on the left side move anteriorly, in a sinistral rotation about the pole, whereas the two on the right also move anteriorly in a dextral rotation about the pole. The two vegetal octants on the left and the two on the right both move posteriorly, similarly in opposing rotations about the vegetal pole.

Interestingly, *Styela* also shows a bilateral symmetry in the classical directions of spiral cleavage (see above). On the right of the embryo, at the third cleavage cycle, the blastomeres are produced to the left, in a vegetal-to-animal direction, and at the fourth cycle they are produced to the right, as in *Nereis*. On the left of the embryo, the blastomeres lie to the right at the third cleavage cycle and to the left at the fourth cycle, opposite to the ways in *Nereis*. Such a change of direction in two quadrants was considered a conceptual link between bilateral cleavage and spiral cleavage (Conklin 1897; see also §4).

We have not drawn attention to the senses of the various offsets in *Styela*, except to those of the third M offsets. The turning couples at offsets described earlier occur in *Styela* but a symmetrical pattern of offsets leads to opposing rotations, rather than synergic rotations as at the third cleavage cycle in *Nereis*. In Conklin's drawings, most offsets are short and so the expected movements would be small. The polar offsets, for example, were sufficiently unremarkable (or variable) for him to have drawn them as dextral or sinistral in different figures. We used the most common version in figure 6*a*.

The senses of the two M offsets at the third cleavage cycle in *Styela* are specific indicators of the bilateral symmetry of the cleavage pattern. The difference between spiral and bilateral cleavage can thus be reduced to the differences in the offsets of the third cleavage cycle. In spiral cleavage, all offsets are the same sense but in bilateral cleavage, the left M offset is dextral and the right M offset is sinistral.

(*d*) *Cleavage in Xenopus laevis*

Our observations of cleavage in *Xenopus laevis* are reported next. We illustrate how variability in the cleavage patterns, which is generally acknowledged to occur (Moody 1987; Dale & Slack 1987), can be documented and related to a representative pattern described in the typic map. Cleavage in *Xenopus* is compared with the bilateral cleavage of *Styela*. In addition, a scheme that names the blastomeres is described for experimental use.

(i) *Methods*

Eggs were stripped from adult female *Xenopus laevis* kept in the laboratory, following previous procedures (Cleine & Dixon 1985). The eggs were fertilized artificially with sperm released by teasing a fragment of an excised testis. Testes were stored in serum at 4 °C and were used as a source of sperm for about one week. Fertilized eggs were kept in 25% modified Ringer (MMR) saline (after Kirschner & Hara (1980) but omitting ethylenediaminetetraacetic acid). The jelly coats were not removed.

Cleavage was watched usually in one or two eggs from each fertilization (named in figure 7)

PHILOSOPHICAL TRANSACTIONS OF THE ROYAL SOCIETY B BIOLOGICAL SCIENCES

under a stereomicroscope. Cleavage was followed up to the 16-cell stage in both the animal and vegetal hemispheres. The fifth cleavage cycle was followed in the animal hemisphere but not to completion in the vegetal hemisphere before the sixth cycle began, and so embryos were fixed in Smith's fixative to preserve the 32-cell stage.

The record of cleavage of a live embryo, made during direct observation under a stereomicroscope, was sufficient to follow the cleavage pattern in the same embryo fixed at the 32-cell stage. The record of cleavage in the vegetal hemisphere for the fifth cleavage cycle was completed by observing the fixed embryo; in addition, the observations made during life were confirmed. The topological maps were then drawn.

(ii) *Results*

The topological maps of *Xenopus* (figure 7) show the lines of the third to fifth cleavage cycles drawn on the left ventral (LV), left dorsal (LD), right dorsal (RD) and right ventral (RV) quadrants. The maps are of 12 embryos up to the 32-cell stage. From these maps, we extracted various datasets to characterize the cleavage pattern. The datasets are the sense of each M and C offset at the second to fifth cleavage cycles and the orientations of the fourth and fifth lines (table 1). We report the features of these datasets (table 2) as follows. At the third cleavage cycle, the M offset on the left of the embryo is dextral (in 10 out of 12 embryos) and that on the right is sinistral (in 12 out of 12 embryos). The orientations of the fourth lines are predominantly parallel to the first line in the ventral animal octants and the dorsal vegetal octants on both the left and right. They are parallel to the second lines predominantly in the remaining octants, namely the dorsal animal octants and the ventral vegetal octants, both left and right. The fifth lines are predominantly parallel to the third lines. In the rest of the data, which are of senses of offsets, there is no dominance of a dextral or sinistral sense in the M offsets at the second cleavage cycle, the C offsets at the third cleavage cycle or the M and C offsets at the fourth and fifth cleavage cycles. Some C offsets of the fifth cycle form within the M offset of the third cleavage cycle. The data are summarized as frequencies in the 12 embryos of characters in the typic map (table 2). The typic map is constructed of the predominant characters in the data and arbitrary choices of non-dominant characters.

The typic map of Xenopus. The typic map (figure 8) is useful as a standard description of cleavage in *Xenopus* against which the extent of the variation in the cleavage patterns in embryos can be documented (table 2). It has bilateral symmetry stemming primarily from the dextral M offset on the left side and the sinistral M offset on the right side at the third cleavage cycle. These offsets are set by the tilts of the third lines in each quadrant. Such tilts were observed by us in *Xenopus* embryos at the time the third cleavage furrows first formed.

Variation of cleavage patterns in Xenopus embryos. The conserved features of the cleavage patterns are the senses of the M offsets at the third cleavage cycle and the orientation of fifth lines parallel to third lines. The mirror-image symmetry of these M offsets is the main source of bilateral symmetry. Somewhat more variable is the orientation of a fourth line and it is probably this that is the source of the generally recognized variation of cleavage in *Xenopus*. A change in the orientation of one fourth line from that in the typic map creates a striking change in the cleavage pattern in polar view. The well-known animal-pole view of a 16-cell embryo (stage 5) in the normal table of *Xenopus* (Nieuwkoop & Faber 1956) deviates from the typic map with respect to the orientation of the fourth line in the left dorsal octant: the line is parallel to the first line, rather than to the second line as in the right dorsal octant.

Similarities between Xenopus and Styela maps. The similarities between the maps of the two

PHILOSOPHICAL TRANSACTIONS OF THE ROYAL SOCIETY B BIOLOGICAL SCIENCES

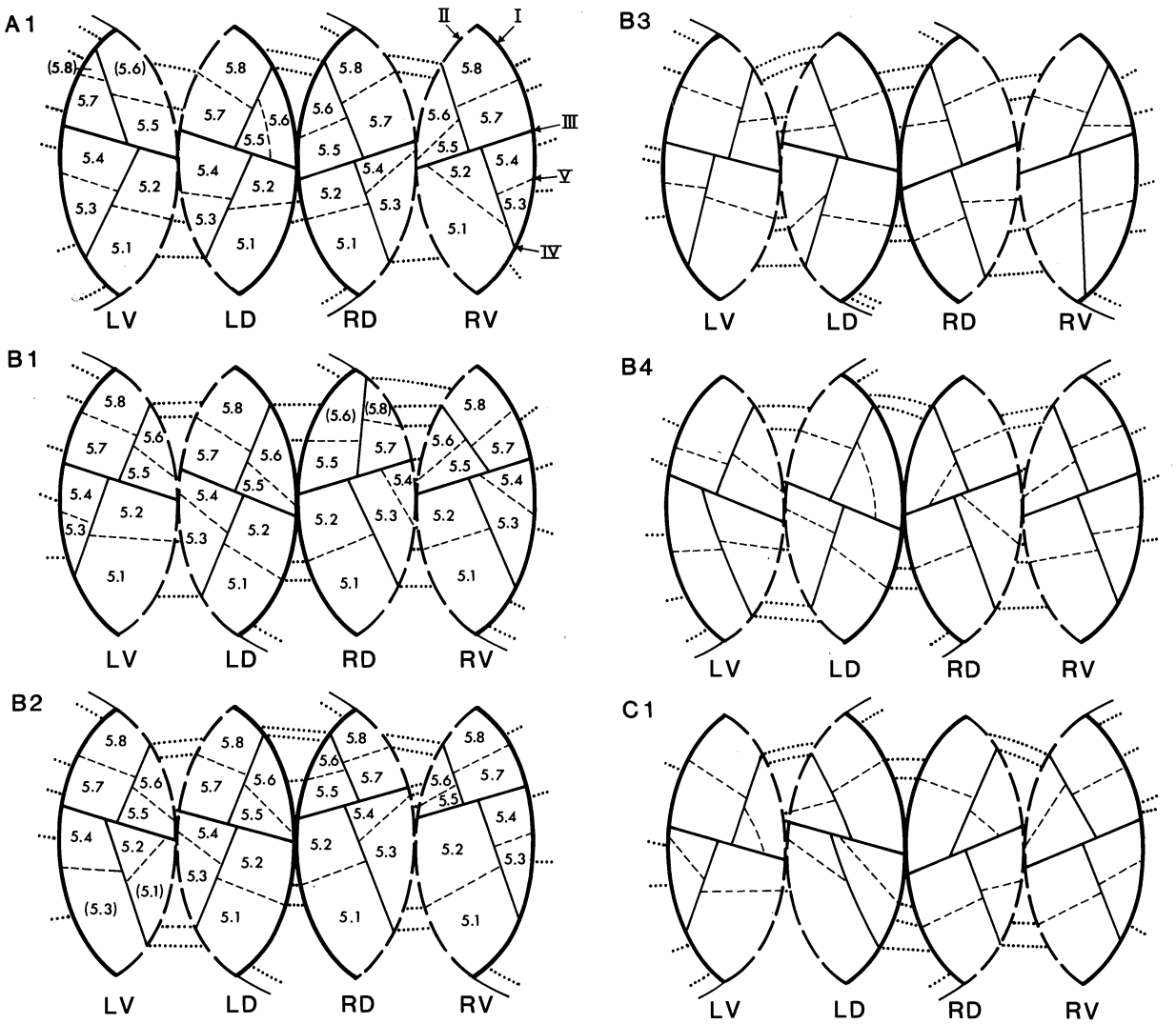

FIGURE 7. For description see opposite.

chordate embryos *Xenopus* and *Styela* centre on the M offsets at the third cleavage cycle. In both maps, the M offsets at the third cleavage cycle are dextral on the left (between LV and LD in *Xenopus* and between A and B in *Styela*) and sinistral on the right (between RD and RV in *Xenopus* and between A and B in *Styela*). The offsets are lateral in both embryos. These mirror-image offsets are the source of the bilateral pattern of symmetry in the *Xenopus* and *Styela* maps. In contrast, little significance can be attached to the senses of the C offsets of the third cleavage cycle.

The orientations of the fourth lines in *Xenopus* (table 2) are mostly the same as in *Styela*. The similarity is not unexpected if the third lines are tilted in the same ways in both embryos and the tilts of third lines determine the orientations of fourth lines. The fifth lines in *Xenopus* and *Styela* are less alike. In our maps of *Xenopus*, the fifth lines have mostly a parallel-to-the-third orientation (table 2). In *Styela*, this is so in the anterior blastomeres.

One notable difference between the maps is in the dorso-ventral and antero-posterior axes.

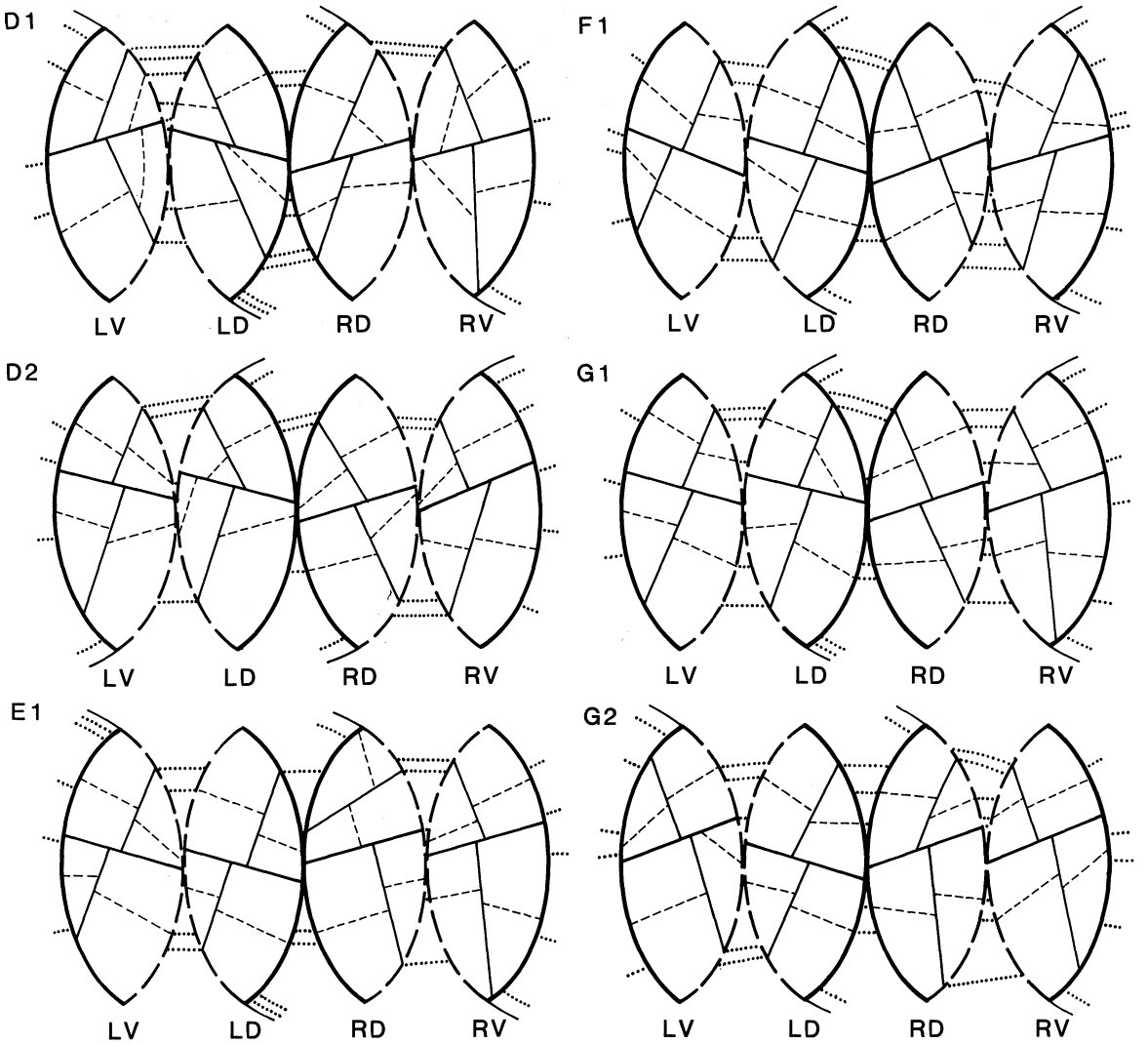

FIGURE 7. Topological maps of 12 embryos of *Xenopus* at the 32-cell stage with animal pole uppermost. The embryos were from seven females named A to G; embryos are named after the female and are distinguished by number. Blastomeres of embryos A1, B1 and B2 are numbered according to a scheme described in figure 9; bracketed numbers indicate departure from the cleavage pattern in the typic map (see figure 9).

TABLE 1. THE TYPES OF DATASET ASSEMBLED IN *XENOPUS*

(The table shows the numbers of datasets assembled at each cleavage cycle. The offsets are either M or C; the orientations are those of the fourth and fifth cleavage lines. At the fourth cleavage cycle, for example, data of four M offsets, two C offsets and eight orientations are tabulated.)

cleavage cycle	offset M	offset C	orientation
first	0	0	0
second	2	0	0
third	2	2	0
fourth	4	2	8
fifth	8	8	8

PHILOSOPHICAL TRANSACTIONS OF THE ROYAL SOCIETY B BIOLOGICAL SCIENCES

TABLE 2. DATASETS IN *XENOPUS* AS FREQUENCIES OF THOSE IN THE TYPIC MAP

(Datasets of the typic map of *Xenopus* are: the senses of M offsets at the second cleavage cycle, the senses of M and C offsets at the third to fifth cleavage cycles and the orientations of fourth and fifth cleavage lines; the number of times the typic value occurred in the maps of 12 embryos are in the bottom row of each subtable. D, dextral; S, sinistral; A, animal hemisphere; V, vegetal hemisphere. The typic map is in figure 8.)

M offsets at the second cleavage cycle[a]

	animal pole		vegetal pole	
	dex.	sin.	dex.	sin.
typic value	0	1	0	1
number of times in 12 embryos	7	5	8	4

M and C offsets at the third cleavage cycle

	M (left)	M (right)	C (ventral)	C (dorsal)
typic value	D	S	S	S
number of times in 12 embryos	10	12	6	7

M offsets at the fourth cleavage cycle

	quadrants			
	LV	LD	RD	RV
typic value	D	D	S	S
number of times in 12 embryos	5	7	7	6

C offsets at the fourth cleavage cycle[b]

	quadrants							
	LV		LD		RD		RV	
	AI	VI	AII	VII	AI	VI	AII	VII
typic value	0	S	0	0	S	0	0	0
number of times in 12 embryos	0	3	4	3	6	1	5	2

M offsets at the fifth cleavage cycle

	quadrants							
	LV		LD		RD		RV	
	A	V	A	V	A	V	A	V
typic value	S	S	S	S	D	D	D	D
number of times in 12 embryos	7	10	6	9	8	10	6	6

C offsets at the fifth cleavage cycle[c]

	quadrants							
	LV		LD		RD		RV	
	AI	VI	AII	VII	AI	VI	AII	VII
typic value	S	S	D	D	S	S	S	S
number of times in 12 embryos	4	5	3	3	3	5	3	8

Orientations of fourth cleavage lines[d]

	quadrants							
	LV		LD		RD		RV	
	A	V	A	V	A	V	A	V
typic value	I	II	II	I	II	I	I	II
number of times in 12 embryos	10	8	8	10	7	11	10	10

Orientations of fifth cleavage lines[e]

	quadrants							
	LV		LD		RD		RV	
	A	V	A	V	A	V	A	V
typic value	III	III	III	III	III	III	III	III
number of times in 12 embryos	10	9	8	9	8	10	11	9

PHILOSOPHICAL TRANSACTIONS OF THE ROYAL SOCIETY B BIOLOGICAL SCIENCES

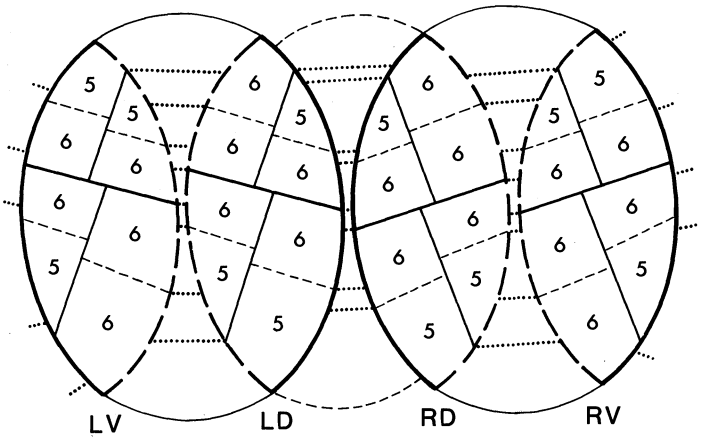

FIGURE 8. The typic map of *Xenopus* at the 32-cell stage with animal pole uppermost. The first and second lines are boundaries of the quadrants, LV, LD, RD and RV. The polar M offsets are sinistral and are chosen arbitrarily. The third line is tilted in each quadrant. The tilt is clockwise from the horizontal in LV and LD and anticlockwise in RD and RV. The tilts make the M offset dextral between LV and LD and sinistral between RD and RV, as predominantly in the data (table 2). The C offsets of the third cleavage cycle, on the first line, are arbitrarily chosen and are made the same sense as the polar offsets so all turning couples act in the same sense along the first line. The sense of the polar offsets also fixes the sense of the C offsets of the fourth and fifth cleavage cycles on the first line (see later). The tilt of the third line sets the orientation of the fourth line in each octant. The fourth line is orthogonal to the third line and thus parallel to the first line in LV and RV animal octants and LD and RD vegetal octants but parallel to the second line in LD and RD animal octants and LV and RV vegetal octants. These orientations are predominant in the data (table 2). The senses of the M offsets of the fourth cleavage cycle are set by an arbitrary decision to partition equally the roughly triangular octants of the 8-cell stage. For example, in the animal octant of LV, the fourth line should meet the third line closer to the first line than to the second to divide the area equally into two; this kind of equal partitioning was described by Thompson (1917). Similarly, the fourth line in the vegetal octant of LV should meet the third line closer to the second line than the first. Such partitioning creates a dextral M offset in LV. Similar arguments lead to a dextral offset in LD but sinistral offsets in RD and RV at the fourth cleavage cycle. The C offsets of the fourth cleavage cycle exist only between the LD and RD animal octants and between the RV and LV vegetal octants on the first line. Their sense is determined by the sense of the polar offsets as said above. Thus in this typic map, the C offsets of the fourth cleavage cycle are both sinistral. The fifth lines are parallel to third lines and so are tilted clockwise in LV and LD and anticlockwise in RD and RV. The orientation of a fifth line is defined by the contacts made by the ends of the pair in each octant. The senses of the M offsets at the fifth cleavage cycle are determined, as at the fourth cycle, by partitioning the triangular areas equally. So the M offsets on the left side are sinistral and those on the right are dextral, in both animal and vegetal octants. The C offsets of the fifth lines on the first line are determined by the sense of the polar offsets. Thus in this typic map, they are all sinistral offsets. The C offsets on the second line are determined by the senses of the M offsets of the third cleavage cycle and are thus dextral between LV and LD and sinistral between RD and RV. The number in each blastomere shows the number of its neighbours.

TABLE 2 (*cont.*)

[a] The sense of the M offset at the animal pole was recorded in 44 other embryos: 18 were dextral and 23 were sinistral and in three the offsets were too small to identify the sense.

[b] The C offsets in the typic map are on only the first line in the dorsal animal octants (AI) and the first line in the ventral vegetal octants (VI) because of the tilts of the fourth lines; AII is the second line in animal octants, VII is the second line in vegetal octants; the C offsets are only recorded once, for the left side of an octant as drawn in figure 8. The occurrences in the 12 embryos are for a C offset irrespective of sense.

[c] AI and VI indicate the offsets on the first line in the animal and vegetal octants respectively and AII and VII indicate those on the second line (see figure 8). C offsets are recorded on only the left side of an octant.

[d] Orientations in the typic map are parallel to the first line (I) or the second line (II).

[e] Orientations in the typic map are parallel to the third lines (III).

According to Conklin, the two inner quadrants of figure 6*a*, A and A are anterior, the vegetal pole is dorsal and the animal pole is ventral. In *Xenopus* (figure 8), the two inner quadrants are dorsal, and essentially, the vegetal pole is posterior and the animal pole is anterior. The two maps can be brought into coincidence by shifting Conklin's axes through 90°, bringing the antero-posterior axis into line with the polar axis by moving the posterior end to the vegetal

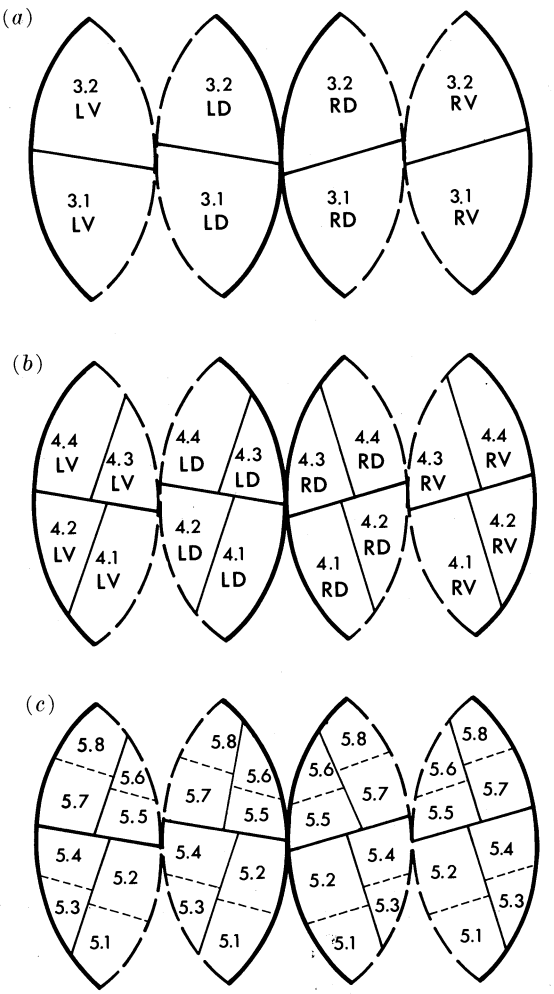

FIGURE 9. Naming scheme for blastomeres in the typic map of *Xenopus*. The first cell is Z (for zygote) and is in generation 0. It divides into L and R for left and right, and they are in generation 1. The four cells of generation 2, formed at the second cleavage cycle, are the quadrants LV, LD, RD and RV (figures 7 and 8). The cells of these first three generations are not shown here. Cells of subsequent cycles have the same number in each quadrant but are identified by the prefix of the quadrant: LV, LD and so on. At the third cleavage cycle (*a*), the cells are 3.1 and 3.2. The number before the point is the generation number and the number after the point identifies cells within a quadrant. The number after the point is higher in cells closer to the animal pole. At the fourth cleavage cycle (*b*), the cells are 4.1, 4.2, 4.3 and 4.4. The generation number is 4 and cell 4.1 is closest to the vegetal pole. At the fifth cleavage cycle (*c*) there are eight cells in each quadrant numbered 5.1 to 5.8; 5.1 and 5.2 are sister cells, as are the next consecutively numbered pairs. The general form of the number is $g.n$, where g is the generation number and $n = 1, 2, 3, \ldots q$, where q is $2^{(g-2)}$, for $g > 2$. The scheme is used to name blastomeres of some embryos in figure 7. Because sister cells are numbered consecutively, the numbering in embryos differs from that in (*c*) if the positions of cleavage lines differ from those in (*c*), which is the typic map. For example, the polar cells in (*c*) are 5.1 and 5.8 at the fifth cleavage cycle. But in the embryos, the polar cells are displaced where fourth-line orientations differ from those in the typic map. This is indicated by bracketing the number of the displaced cells (figure 7, embryos A1, B1, B2). The bracketing is a useful indication of departure from the typic map in an observed cleavage pattern.

PHILOSOPHICAL TRANSACTIONS OF THE ROYAL SOCIETY B BIOLOGICAL SCIENCES

pole. The major axes in the maps are then the same. That it is reasonable to shift the axes in this way, we suggest, is because the blastopore in *Styela* is at the vegetal pole and a blastopore is generally regarded as posterior. The anterior lip of the blastopore in *Styela* (Conklin 1905) would become the dorsal lip, as in *Xenopus*.

Notwithstanding the arguments for rotating the axes named by Conklin through 90°, a change in nomenclature is not recommended because of established usage in developmental studies of ascidian development. The argument is made here to show the similarity between the cleavages of two chordates widely separated in the phylogenetic classification.

Naming blastomeres in Xenopus. The scheme proposed for naming blastomeres in *Xenopus*, explained in figure 9, is based on Conklin's scheme for *Styela*. In our scheme, however, the first cell is in generation 0 and so the number preceding the point (figure 9), which is the generation number, is always one less than in Conklin's scheme. Our generation number when made an exponent of 2 gives the total number of cells in the embryo. It is also the number of the last cleavage cycle that took place.

The type of cleavage in Xenopus. Cleavage in *Xenopus* has been described as bilateral, yet it is often drawn as the classic orthoradial type named by Conklin (1897). There, meridional cleavage lines are intersected by other lines at right angles and lines meet at four-radiate junctions. Conklin believed the orthoradial type to be rare or at best short-lived. Yet it is how cleavage in *Xenopus* is treated in experimental studies (Nakamura & Kishiyama 1971; Hirose & Jacobson 1979; Dale & Slack 1987). The junctions in *Xenopus* embryos are usually three-radiate and the pattern at the 32-cell stage is more like a cap of four blastomeres at the poles and three tiers of eight blastomeres between the poles. The four blastomeres can be made out forming a cap or a cross at the animal pole in a 32-cell stage *Xenopus* embryo. A similar group of four blastomeres is found at the poles in a 32-cell stage in *Styela* (Conklin 1905).

3. Partitioning the plane into polygons with six neighbours

We come now to the question of whether the forms of cleavage patterns can be explained. The hypothesis we explore is that cleavage patterns are ways of partitioning the cytoplasm that lead to embryonic epithelia where cells have six neighbours, a partitioning generally accepted as a natural form of cellular arrangement (Thompson 1917). To this purpose, we describe ways of dividing two-dimensional space into polygons with six neighbours by lines drawn sequentially. We then compare cleavage in embryos with this partitioning.

The sequential partitioning results in polygons that we define as N-gons, where N is the number of neighbours of a polygon. For simplicity, we draw the explanatory figures on an orthogonal lattice and note only the number of neighbours of a polygon, ignoring the number of its geometric sides. The number of sides is not of interest because a new division line would deform the existing line it met, and no angle at a meeting point (vertex) would remain at 180°, so the number of sides of a polygon would equal the number of neighbours (Cowan & Morris 1988). All vertices in the partitioning are three-radiate, that is, they have three lines emanating from them. This is a consequence of partitions in neighbouring polygons being offset, not meeting at a four-radiate junction as specified initially in the general scheme.

We describe first a simple construction for partitioning the plane into 6-gons by lines drawn sequentially and then a variation, the reflected line, that also leads to 6-gons.

PHILOSOPHICAL TRANSACTIONS OF THE ROYAL SOCIETY B BIOLOGICAL SCIENCES

(*a*) *Partitioning the plane*

(i) *The simple construction for* 6*-gons*

The simple construction is drawn in figure 10: the partitioning there leads to a mosaic of 6-gons over the infinite plane. The lines simulate successive cleavage cycles and are orthogonal to each other. The first line is a thick vertical line that partitions the plane into left and right. The second lines, which partition left and right into upper and lower areas, are dashed and meet the first line at a sinistral offset. The third lines are vertical and meet the second lines at dextral offsets. The fourth lines are again horizontal and meet third lines and the first line at sinistral offsets. The partitioning could be continued with alternate vertical and horizontal lines dividing the columns and rows of polygons without intersecting existing offsets, which are conceptually very small. The rule for generating 6-gons in this figure is that horizontal lines meet each existing vertical line at an offset of the same sense, the sense of the first offset. Vertical lines meet each existing horizontal line at an offset of the same sense, but opposite to that of the first offset. The first offset thus determines the senses of all subsequent offsets.

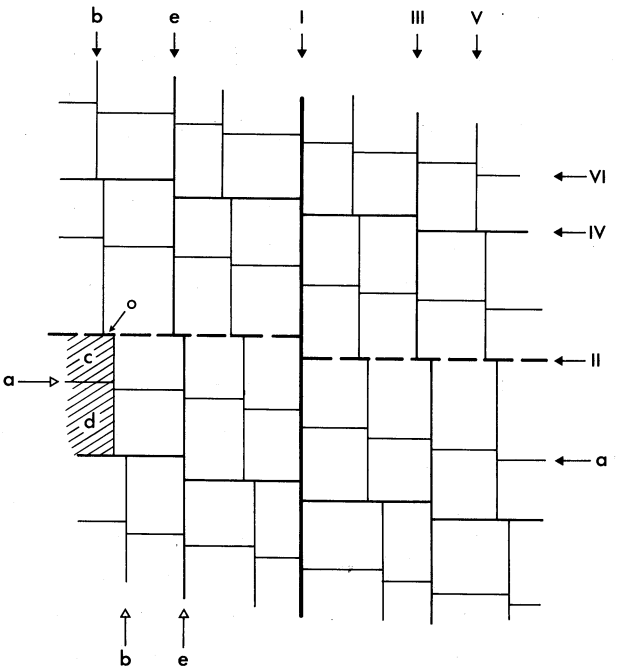

FIGURE 10. Partitioning of the plane leading to 6-gons: the simple construction (see text). Partitioning is by division lines simulating the first to sixth cleavage lines (I to VI). All offsets on vertical lines are sinistral, all those on horizontal lines are dextral. Line a enters the plane and crosses line b; it excludes the offset from polygon c (with an existing offset, o) but includes it in polygon d (without an existing offset); the same rule applies when line a crosses line e.

The lines of one cycle can be imagined to be laid down simultaneously, or to proceed across the plane dividing each polygon in turn. For any line of the third or later cycles crossing the plane, a rule that preserves 6-gons is one that places the two offsets in each polygon at opposite corners, as in figure 10. Such a rule is shown in figure 10: line a when crossing existing line b excludes the offset from polygon c, which has an offset at the adjacent corner, and puts it in polygon d, which has not. The same exclusion happens when line a crosses line e. The result is that all offsets created by line a are sinistral. We call it the exclude-offset rule.

PHILOSOPHICAL TRANSACTIONS OF THE ROYAL SOCIETY B BIOLOGICAL SCIENCES

(ii) *The reflected line*

The exclude-offset rule, even so, is not mandatory for generating 6-gons. If the first offset breaks the rule, the situation can be rescued by breaking the rule at all subsequent intersections giving all offsets in that line the same sense (figure 11*a*, line b). The new line is the mirror-image of a line that obeys the exclude-offset rule and is called a reflected line. The reflected line creates polygons in which offsets are on adjacent corners (figure 11*a*, shaded polygons), not on opposite corners. A line orthogonal to it would divide one such polygon into a 4-gon and a 6-gon: so to maintain 6-gons, both new offsets must be in the 4-gon. The lines of the next cycle thus have no choice of sense of offset when they enter the partitioned plane, if 6-gons are to be maintained (figure 11*b*, asterisked lines).

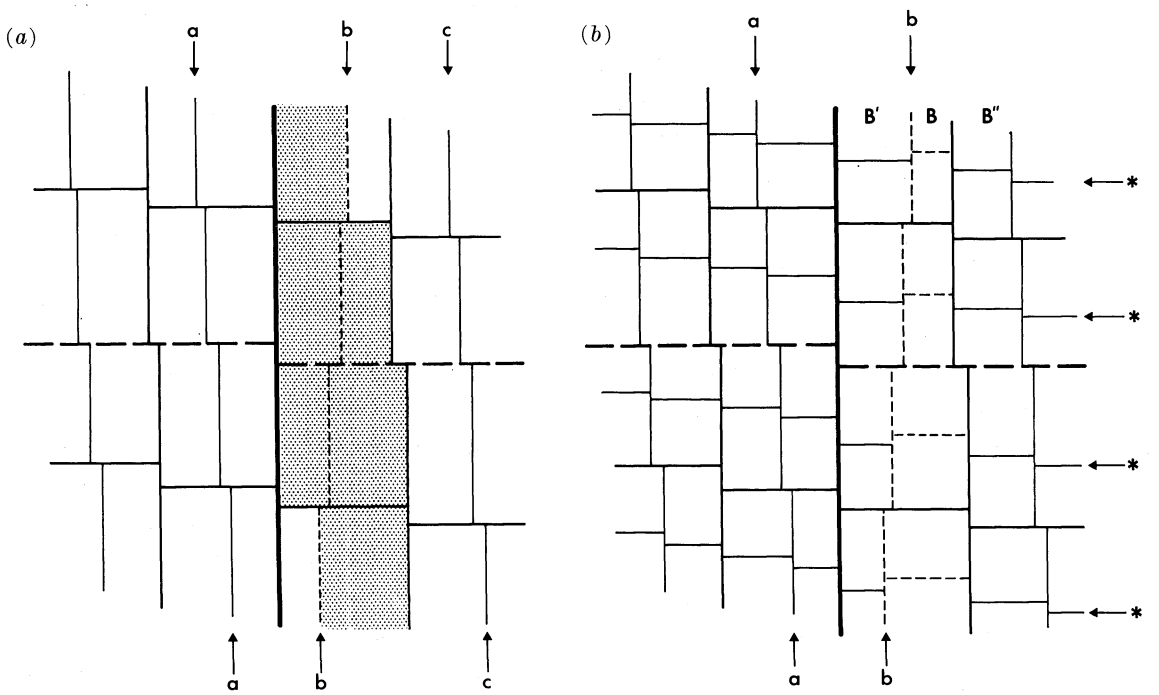

FIGURE 11. Partitioning of the plane leading to 6-gons: the reflected line (see text). (*a*) After five cycles of division lines. Line b is a mirror-image reflection of lines a and c; shaded polygons have offsets on adjacent corners. (*b*) After six cycles of division lines. The offsets made by sixth lines (asterisked), which are orthogonal to line b, are determined; polygons in columns B′ and B have offsets on adjacent corners; 6th lines are elevated in column B relative to lines in B′ and B″.

In fact, lines of all cycles orthogonal to a reflected line after it is formed have determined senses of offsets, if 6-gons are to be made. These senses are as in the simple construction on non-reflected lines but opposite to this sense on the reflected line. This is shown in figure 11*b*.The horizontal lines identified by asterisks make sinistral offsets where they cross non-reflected vertical lines and dextral offsets where they cross the reflected line labelled b. This change to dextral must occur in all future horizontal lines because polygons with offsets on adjacent corners, those in columns B and B′ (figure 11*b*), have become a permanent feature of the partitioning. All *vertical* lines still have a choice of sense of offset when they enter the partitioning. Should any of these be a reflected line, the determined horizontal lines that follow just reflect from the simple-construction sense of offset as they cross the new reflected line, to preserve 6-gons.

So, any vertical or horizontal line entering a simple construction has a choice of sense of offset. Once chosen, all offsets in the remainder of the line must be the same as the first choice. If a reflected line is created, only lines parallel to it have a choice of sense of offset.

(iii) *Procedures for* 6*-gons*

To summarize, 6-gons are created in sequential partitioning when all offsets on vertical lines are of like sense and all offsets on horizontal lines are of like sense but opposite to those on vertical lines; this is the simple construction. In a reflected line, all offsets are reversed from the simple construction. Offsets in lines of subsequent cycles orthogonal to it are determined and they are reflected with respect to the simple construction when the reflected line is crossed. In other words, offsets made on a reflected line should be of opposite sense to those made by the reflected line itself. These procedures for 6-gons are for the situation where all polygons divide at each cycle.

(*b*) *Partitioning a sphere*

The rules for 6-gons, described for the plane, apply also to sequential partitioning of a sphere because partitioning in the plane can be transferred to a sphere. We describe this transfer now for the simple construction for 6-gon partitioning.

First, boundary lines are added to the plane. They are drawn first as a vertical and a horizontal segment in each quarter of the plane (figure 12*a*). They follow the rules of the simple construction. They make offsets where they meet at first and second lines and offsets are made on them where other lines cross them, in accordance with the rules (figure 12*a*). This partitioning is transferred to a sphere by first joining the vertical and horizontal segments at the corners to form complete boundary lines (figure 12*a*). These boundary lines become curved, creating a stepped disc (figure 12*b*). The disc via a change of shape becomes a hemisphere and a replica of itself translates meridionally to the position of the other hemisphere. The two hemispheres fuse along their boundary lines, forming a sphere. The offsets on the boundary lines will fuse if they are of like sense, which they will be if the rules for the simple construction have been followed. The fused boundary lines have vertical and horizontal properties with respect to offsets because they are made in part of a vertical segment and in part of a horizontal segment. Where the vertical and horizontal segments join in each quarter, the polygon formed is not a 6-gon. We call such polygons the residual polygons (figure 12*b*). There are always eight in the partitioned sphere. They are remnants of the eight faces of the octagon formed by the three primary planes (figure 1).

The 6-gon partitioning containing a reflected line can also be transferred to a sphere, but there are constraints when making the sphere. If a vertical line is reflected (figure 12*c*), the direction of the meridional translation of the replicate hemisphere must be parallel to the vertical line when making the sphere, so that the offsets that are to fuse are of like sense. The replica cannot translate orthogonally to the reflected line because the offsets would not match. If a horizontal line is reflected, the direction of translation of the replica must be parallel to the horizontal line. We point out that the vertical or horizontal part of a boundary line between two residual polygons can itself be a reflected line and that the direction of translation of the replicate hemisphere must again be parallel to the reflected part. So, for a sphere, a reflected line is parallel notionally to a meridian or to the equator or it is the boundary line between residual polygons.

Using these findings, we can transfer the cleavage pattern of an embryo to partitioning in

PHILOSOPHICAL TRANSACTIONS OF THE ROYAL SOCIETY B BIOLOGICAL SCIENCES

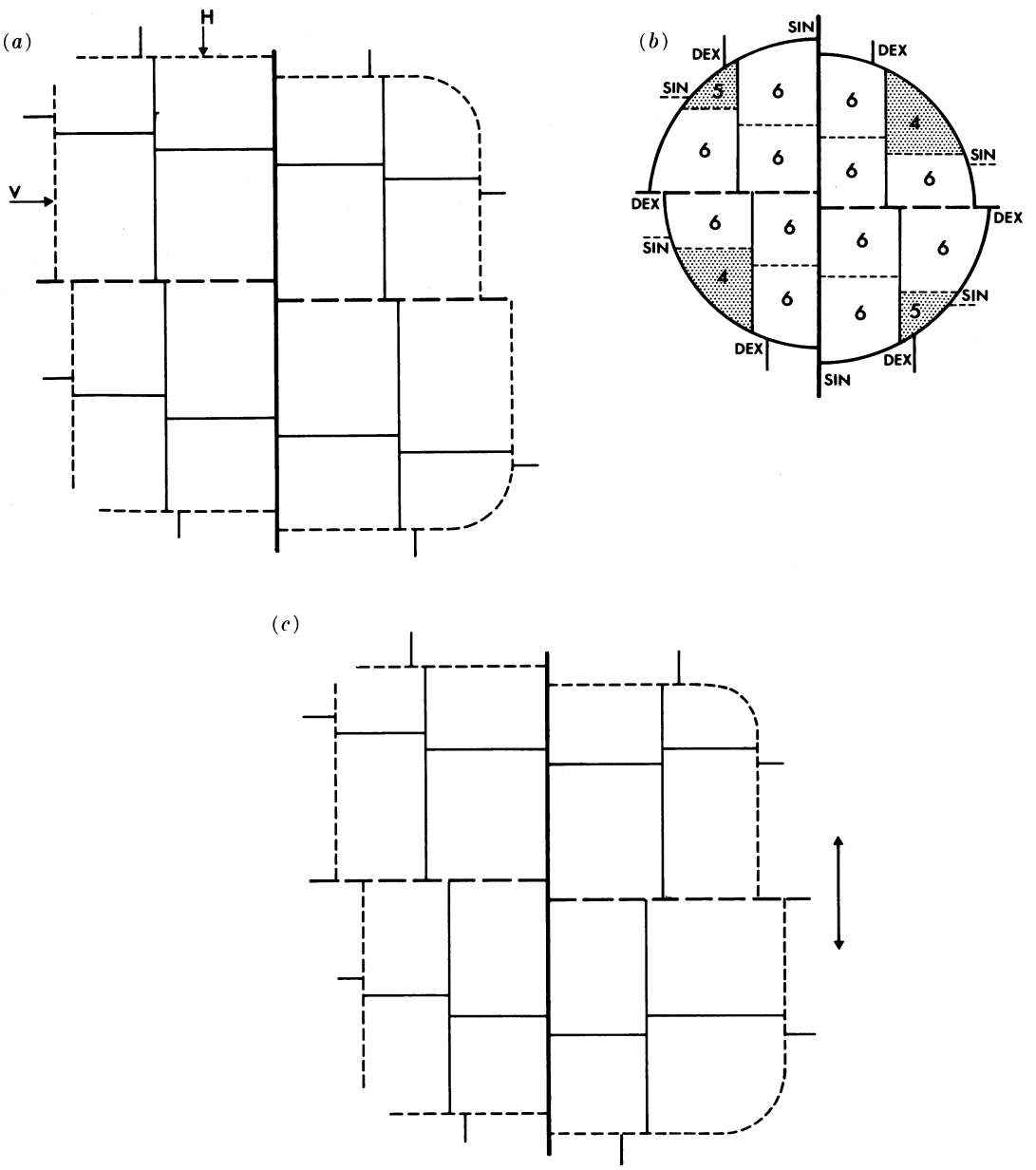

FIGURE 12. Steps in the transference of partitioning in the plane to a sphere. (*a*) Boundary lines (dashed) are added to the partitioning. They are shown as vertical (V) and horizontal (H) segments on the left but on the right they are joined at the corners; offsets are sinistral where division lines cross the vertical segments but dextral where they cross the horizontal segments. (*b*) The stepped disc formed when joined boundary lines become curved. Offsets on the boundary lines are sinistral (SIN) or dextral (DEX) depending on whether they are on the vertical or horizontal segments of the now continuous boundary lines. Polygons either side of the first line and either side of the second line are 6-gons. The residual polygons (shaded) are 4-gons or 5-gons and are formed where the vertical and horizontal segments of boundary lines join. (*c*) Similar to (*a*) but with a reflected line on the right. To form a sphere, a replica of the figure must translate meridionally in a direction (double-headed arrow) parallel to the reflected line, so the offsets destined to fuse are of like sense.

PHILOSOPHICAL TRANSACTIONS OF THE ROYAL SOCIETY B BIOLOGICAL SCIENCES

the plane. The pattern of offsets can then be compared with that in the simple construction and reflected line.

(*c*) *Cleavage patterns drawn as orthogonal lattices*

In transferring the cleavage pattern of an embryo to the plane, segments of the primary cleavage lines become boundary lines. The primary cleavage-line segment that becomes the boundary line in a particular octant is the one to which the fourth and fifth lines are not parallel. For example, if the fourth and fifth lines are parallel to the first and third lines, the second line becomes the boundary line. Each boundary line is divided into a vertical and horizontal segment and so behaves in part as a vertical line and in part as a horizontal line with respect to offsets. In the descriptions that follow, the cleavage patterns are constructed of octants whose boundaries are determined in these ways. The descriptions illustrate the merits of this technique.

(i) *Cleavage of Nereis as an orthogonal lattice*

The cleavage of *Nereis* in figure 3*e* is drawn as an orthogonal lattice in the plane in figure 13. The lattice is constructed of octants, which are fused to form the quadrants A, D, C and B. In A, the boundary line in the animal octant is the second line because the fourth and fifth lines are parallel to the first and third lines; it is divided into vertical and horizontal segments. In the vegetal octant of A, the boundary line is the first line because the fourth and fifth lines are parallel to the second and third lines and it is similarly divided. The boundary lines of the remaining octants are determined similarly. The line segments fuse where they are common.

In the orthogonal lattice (figure 13), the similarity of the pattern of offsets between quadrants and the unique cleavage of the d^2 blastomere are clear. Some fifth lines meet at C offsets within the M and C offsets of the third cleavage cycle. This is commented on below.

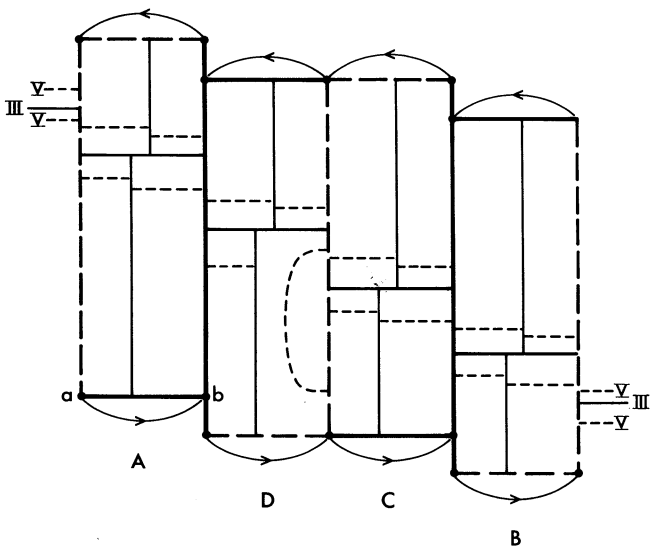

FIGURE 13. Cleavage in *Nereis* (figure 3*e*) drawn as an orthogonal lattice (see text). The orthogonal lattice is converted back to a sphere by compressing each horizontal segment of the first and second lines into the vertical segment. For example, the line ab slips through the point at b until point a is coincident with b. The vegetal end of a second line (point a) is then at one end of the vegetal polar offset and the fourth line joins a wholly vertical first line. The other horizontal segments are compressed in the directions of the arrows. The sphere is formed when the second line in A fuses with that in B. The polar offsets are steps on the first line.

PHILOSOPHICAL TRANSACTIONS OF THE ROYAL SOCIETY B BIOLOGICAL SCIENCES

(ii) *The typic map of Xenopus as an orthogonal lattice*

The typic map of *Xenopus* (figure 8) is drawn as an orthogonal lattice in figure 14. In the animal octant of LV, the boundary line is the second line. In the vegetal octant of LV, the boundary line is the first line. In each of these octants, the boundary line is formed from the primary line segment to which the fourth and fifth lines are not parallel. The boundary lines are divided into vertical and horizontal segments. The boundary lines in the remaining octa are determined similarly.

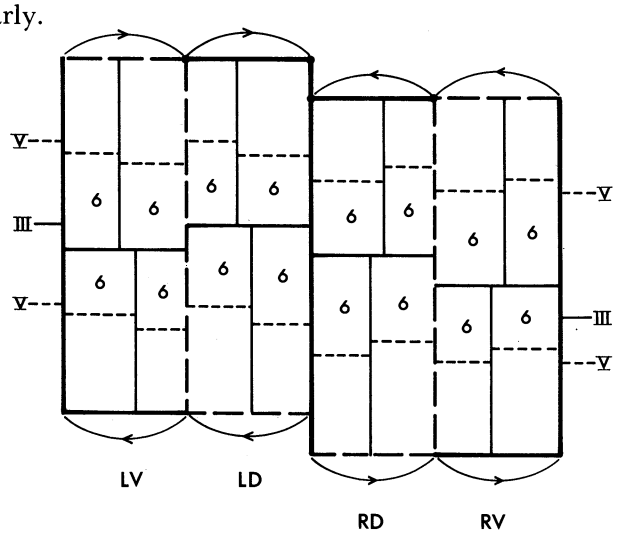

FIGURE 14. Cleavage in the typic map of *Xenopus* (figure 8) drawn as an orthogonal lattice (see text). The blastomeres either side of the third lines, labelled 6, each have six neighbours. Arrows, as in figure 13, indicate the directions in which horizontal segments should be compressed to convert the orthogonal lattice to a sphere.

There are two rows of 6-gons, one each side of the third lines (figure 14). The 6-gons in RD and RV are constructed from reflected fourth lines and reflected M offsets of fifth lines, given that sinistral is the sense of offset on vertical lines in the simple construction, it being set by the polar offsets. In the left quadrants, only the third M offset is reflected; the four cells around it are 6-gons because the C offsets of the fifth lines on the second line are dextral also. The reflection of the third M offset to dextral in the left quadrants is the reflection that first gives bilateral symmetry to the cleavage pattern. The other reflections that contribute to bilateral symmetry are those of the fourth and fifth M offsets on the right of the embryo.

(*iii*) *Cleavage of a Xenopus embryo as an orthogonal lattice*

Cleavage in a *Xenopus* embryo is drawn as an orthogonal lattice (figure 15) for embryo B2 of figure 7, by using the same procedure. The lattice shows the reflections and the deviations from the rules of 6-gon partitioning. The polar offset is dextral in this embryo and so dextral is the form for offsets on vertical lines in the simple construction. Thus the third M offset between RD and RV, which is sinistral, is reflected from the simple construction, as is the third C offset between RV and LV. Of the fourth M offsets, the dextral offset in LD is reflected from the simple construction and the sinistral offset in RD is a reflection from the requirement that an offset on a reflected line should itself be reflected. These reflected M offsets are labelled in figure 15. Of the fifth M offsets, four are reflected with respect to our rules. These are the sinistral offsets labelled S in LV and the dextral offsets labelled D in RV.

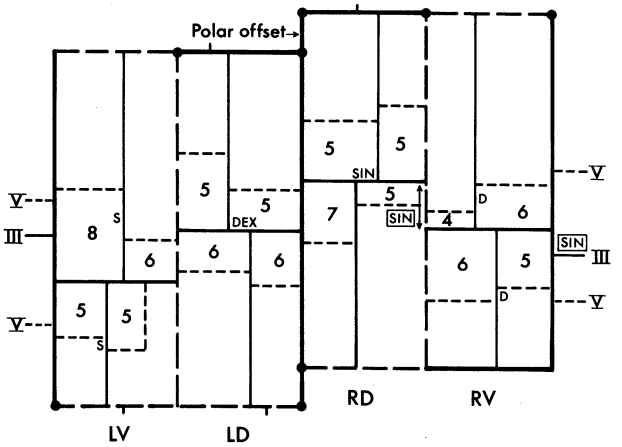

FIGURE 15. Cleavage in a *Xenopus* embryo (figure 7, embryo B2) drawn as an orthogonal lattice (see text). All reflected M offsets are labelled: those of the third cleavage cycle are labelled SIN (boxed), those of the fourth cycle are labelled SIN or DEX and those of the fifth cycle are labelled S or D, according to their sense. The numbers are the number of neighbours of a blastomere. In the LV vegetal octant, the third line is the boundary line but it is not represented as such because it is not common with the vertical segment of the boundary line in the LD vegetal octant.

The pattern of offsets determines the numbers of neighbours of blastomeres. In the 16 blastomeres either side of the third lines (figure 15), only five are 6-gons because of the deviations from our rules. The lattice has bilateral symmetry. The third M offset between RD and RV, sinistral in sense, begins the symmetry. The fourth M offsets in the left quadrants are mirror-images of those on the right, as are the fifth M offsets on the left and the right. The fourth line in the vegetal LV octant, however, is parallel to the first line.

Some C offsets lie within an offset formed at a previous cleavage cycle. In particular, the fifth C offset between the animal octant of LV and the vegetal octant of LD lies within the third M offset between LV and LD. This offset is sinistral within the dextral third M offset and the two blastomeres there are 6-gons. A similar fifth C offset lies within the third M offset between RD and RV. Here, a sinistral offset lies within another sinistral offset and the two blastomeres there are not 6-gons. This feature of an offset lying within a previously formed offset also occurs in *Nereis*. It is not allowed in the simple construction and reflected line (figures 10 and 11) but we shall accommodate it later.

In the *Xenopus* embryos, various deviations from the rules of the simple construction and reflected line lead to variations in the numbers of neighbours of blastomeres. In table 3, we give the distribution of neighbours of blastomeres in the 12 embryos examined, as well as the distribution for 6-gon partitioning on a sphere for 32 polygons including the residual polygons, which have less than six neighbours. In the embryos, there are blastomeres with seven neighbours but few with more than this. The number of blastomeres with four neighbours is less than for 6-gon partitioning. There is some evidence of bias against the lower and higher classes of numbers of neighbours.

(iv) *Cleavage of Styela as an orthogonal lattice*

Cleavage in *Styela* (figure 6*a*) is drawn as an orthogonal lattice in figure 16. The pattern in *Styela* is similar to that in the *Xenopus* embryo B2 (figure 15) up to the fourth cleavage cycle. In *Styela*, the pattern at the fifth cleavage cycle within the left quadrants B and A is the mirror-

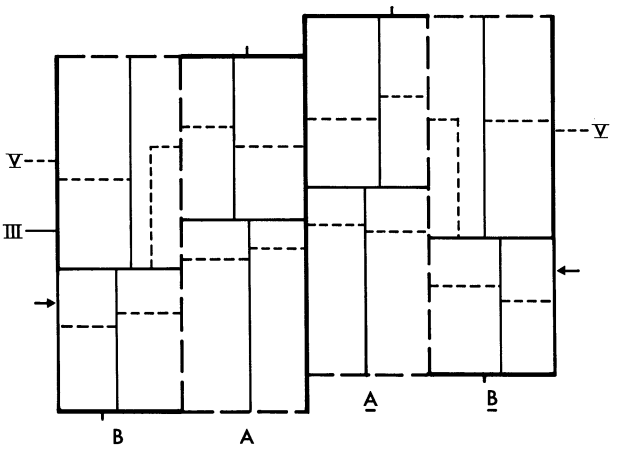

FIGURE 16. Cleavage in *Styela* (figure 6*a*) drawn as an orthogonal lattice. In the vegetal octants of B and B, the boundary lines are third lines (arrows label vertical segments), rather than segments of first and second lines as in the other octants.

TABLE 3. NUMBERS OF NEIGHBOURS OF BLASTOMERES IN *XENOPUS*

(Numbers of blastomeres at the 32-cell stage with three to nine neighbours; data from cleavage maps of the 32-cell stage in 12 embryos of *Xenopus* in figure 7. Numbers of polygons with three to nine neighbours in 12 spheres each partitioned into 32 polygons according to the simple construction are given for comparison. The numbers of neighbours in the typic map are also shown.)

	numbers of neighbours						
embryo name	3	4	5	6	7	8	9
A1	0	1	15	11	5	0	0
B1	0	1	15	11	5	0	0
B2	0	1	15	12	3	1	0
B3	0	2	10	18	2	0	0
B4	0	1	13	16	1	1	0
C1	1	5	7	13	5	0	1
D1	0	4	12	9	6	1	0
D2	0	3	9	17	3	0	0
E1	0	1	15	11	5	0	0
F1	0	1	14	13	4	0	0
G1	0	2	12	15	2	1	0
G2	0	2	13	13	3	1	0
total	1	24	150	159	44	5	1
total in 12 spheres	0	48	48	288	0	0	0
typic map	0	0	12	20	0	0	0

image of that on the right in A and B. The polar offsets and other offsets on the first line between A and A and between B and B, of course, do not share the mirror-image symmetry.

(v) *Conclusions*

By drawing cleavage patterns as orthogonal lattices we can compare them with the 6-gon partitioning described earlier in this section. How far they conform to the rules of 6-gon partitioning and how the number of neighbours about each blastomere is arrived at can then be investigated. Examples of conformity to 6-gon rules are the alternations in the senses of offsets in successive cycles, as happens in the fourth and fifth cycles in the dorsal quadrants of a *Xenopus* embryo (figure 15). A reflected line is utilized in the bilateral form of cleavage in

PHILOSOPHICAL TRANSACTIONS OF THE ROYAL SOCIETY B BIOLOGICAL SCIENCES

Xenopus and *Styela*. On the other hand, the pattern of sinistral offsets in *Nereis* cannot lead to 6-gons and this is evident in figure 13. Incorrect offsets reduce the number of 6-gons in the *Xenopus* embryo B2 and to some extent in *Styela*. But on balance, the patterns have bias towards 6-gons.

(*d*) *General procedures for* 6-*gons*

The problem addressed above is how a lattice of polygons, each with six neighbours, maintains polygons all with six neighbours at the end of every cycle of divisions. It is a problem of the division of space sequentially and applies to cell divisions. We have given a method for maintaining a 6-gon lattice after every cycle of divisions, but interestingly the cleavage patterns in embryos exhibit a feature not allowed in our procedures. This is the offset that is made within a previously established offset. We explore now a general procedure for 6-gon partitioning that includes offsets made within existing offsets.

(i) *A general rule for* 6-*gons*

The offset that is formed within an existing offset is not used in the orthogonal lattice (see figures 10 and 11) that gives 6-gon partitioning. The orthogonal lattice limits the faces of a 6-gon that a division line may contact and is useful to the extent that the sequential division lines can be displayed *ad infinitum* in a simple way. The faces of the 6-gon that a division line contacts in the simple construction are the opposite faces (figure 10), because every 6-gon is divided into two 5-gons [5, 5]. Where an offset is formed within an existing offset, a 6-gon is divided into a 4-gon and a 6-gon [4, 6] (figure 17*a*) and the division line is between two nearest non-adjacent faces of the 6-gon. To preserve 6-gons here, each division line in the neighbouring 7-gons must contact the 4-gon (figure 17*b*). It is clear that the offset formed within an offset must be of the opposite sense to the one in which it lies if 6-gons are to be preserved (figure 17*b*). When this situation is represented on a hexagonal lattice (figure 18*a*), we see that an offset within an offset shifts the partitioning into an adjacent row of the lattice, because of the [4, 6] division. If all cells in such a lattice are to divide, those in neighbouring rows must also shift their row when they divide to maintain 6-gons. In a similar way, the [4, 6] divisions of polygons either side of a reflected line (figure 11*a*, *b*) also involve a shift to an adjacent row in a hexagonal lattice (figure 18*b*).

The general rule is that division lines may pass through a hexagonal lattice, as in figure 18*a*, dividing each newly made 7-gon into [5, 6] but with the new offset raising the 5-gon of the previous 7-gon division to a 6-gon. The division lines may pursue an irregular path because there are two ways of dividing the 7-gon into [5, 6]. If all cells in the lattice are to divide once, other division lines must follow alongside the path of the first set of division lines.

We have explored further the orientations of division lines in a hexagonal lattice and found there can be some random choices of orientation in division lines, between opposite faces of the hexagon, that divide the lattice yet still preserve 6-gons after each cycle of divisions. We do not report these results here except to say the orientations of division lines in pairs of adjacent cells can be reduced to two types. Using the terminology of Abbott & Lindenmayer (1981), who named the division patterns described by Korn & Spalding (1973) and Lewis (1926), we call them a Korn–Spalding tetrad (KS tetrad) and a Lewis tetrad (L tetrad) (figure 19). In the KS tetrad, the division lines have the same orientation in both cells but in the L tetrad the division lines are at an angle to one another and, of course, the KS and L tetrads each exist in two forms (figure 19); the KS tetrad can have a dextral offset (D-form) or a sinistral offset (S-form)

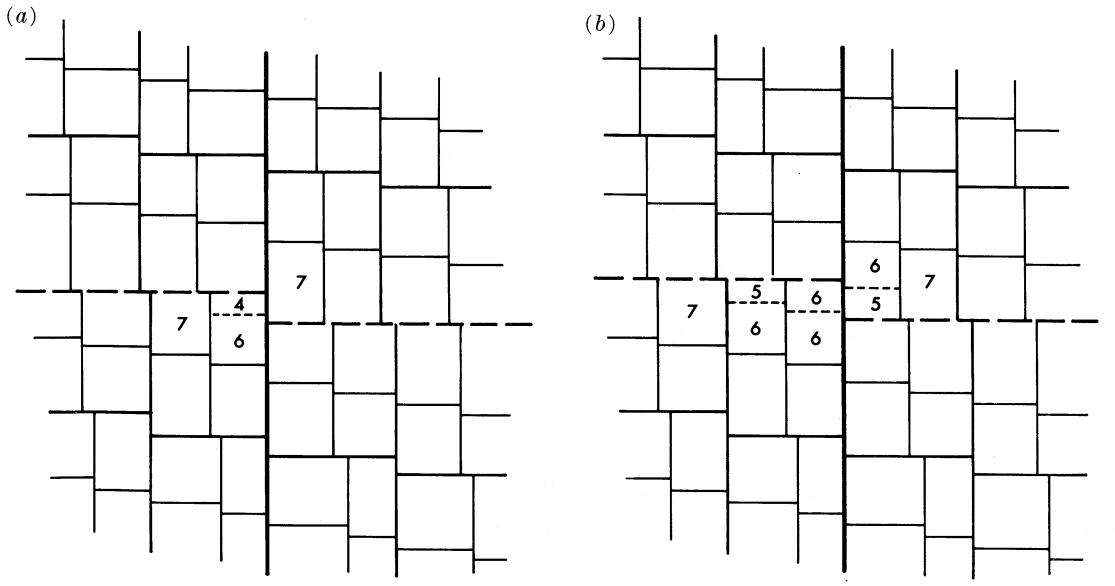

FIGURE 17. The offset formed within an existing offset. In (*a*) the division line (dashed) divides a 6-gon into [4, 6]. The 7-gons in (*a*) have divided in (*b*) into [5, 6] creating two new 7-gons and raising the 4-gon in (*a*) to a 6-gon. The offset formed within the existing offset is dextral, opposite in sense to the existing offset; thus to preserve 6-gons an offset within an offset must be of the opposite sense to the existing offset.

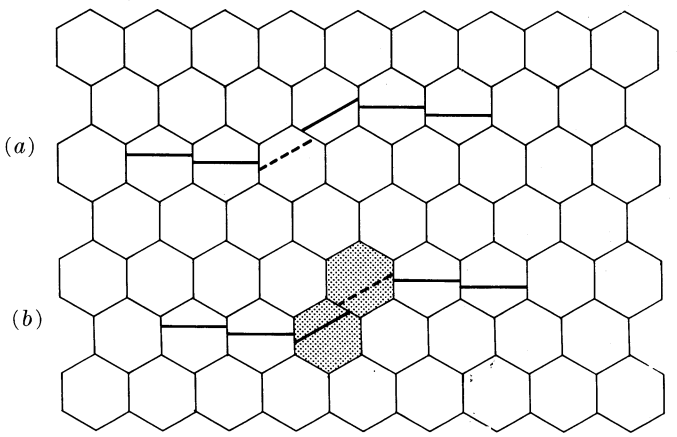

FIGURE 18. Division lines drawn on a hexagonal lattice. (*a*) The offset within an existing offset is initially a [4, 6] division (dashed line) that makes one new 7-gon in an adjacent row (compare with figure 17*a*); a similar [4, 6] division of a hexagon allows divisions to proceed in the adjacent row. (*b*) Divisions that cross a reflected line (see figure 11*b*) are similarly two successive [4, 6] divisions that in a hexagonal lattice shift between adjacent rows; the shaded polygons correspond to either of the pairs of shaded polygons in a row in figure 11*a*; the dashed line corresponds to any horizontal dashed line in column B in figure 11*b*.

corresponding respectively to the S and Z forms of Lindenmayer (1984). The simple construction of 6-gon partitioning (figure 10) is made up of KS tetrads and it is clear that the merit of this tetrad in forming 6-gons, in contrast to the L tetrad, is the reciprocal behaviour of the division lines. One end of each division line contacts the other dividing cell and thus immediately restores two of the four daughter cells to 6-gons. In the L tetrad, only one of the four daughter cells is restored to a 6-gon. Where cleavage lines in sister cells contact their

PHILOSOPHICAL TRANSACTIONS OF THE ROYAL SOCIETY B BIOLOGICAL SCIENCES

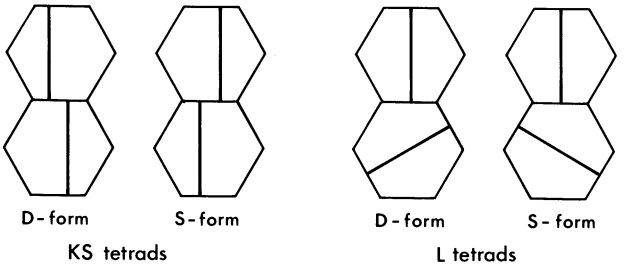

FIGURE 19. The forms of KS tetrad and L tetrad that constitute the pattern of divisions in a hexagonal lattice that preserves 6-gons (see text).

mother-cell membrane forming an M offset, they create a KS tetrad. It is a division pattern that has more chance of preserving six neighbours around cells in a dividing epithelium.

Another situation is where not all cells in the lattice divide. In essence, this allows more freedom in how division lines orient if 6-gons are to be kept, than where all cells divide in each cycle.

(ii) *The lattice in which* 6*-gons are not preserved*

Other matters bear on sequential divisions in a polygonal lattice. We know for a lattice in the infinite plane (Cowan 1978), if all vertices are three-radiate, the average number of neighbours per polygon is exactly six. So when a 6-gon in an otherwise 6-gon lattice divides [5, 5], the two 7-gons created keep the average at exactly six. Similarly, a [4, 6] division, or even a [3, 7] division, implies two 7-gons in the lattice to keep the number of neighbours about each polygon at an average of six. If in a series of sequential divisions 6-gons are not maintained, the average N-gon value in a planar lattice is still six. For a lattice on the surface of a sphere, having three-radiate vertices, the average number of neighbours of a polygon is less than six. Following Euler, we have the mean number of neighbours per polygon on the surface of any solid topologically equivalent to a sphere, $\mu = 2\theta(F-2)/(\theta-2)F$, where θ is the mean number of arms at a vertex and F is the total number of polygons; if $\theta = 3$, $\mu <$ six. Lewis (1943) pointed out there were twelve pentagons on a solid surface otherwise covered by hexagons. The residual polygons created in making a sphere are explained: these are the four pairs of 4-gons and 5-gons in a lattice otherwise composed of 6-gons, that account for the shortfall of 12 neighbours. There can be no more than 24 blastomeres with six neighbours in a 32-cell embryo (table 3).

4. DISCUSSION

We have analysed early cleavage patterns topologically and simplified them into a stylized projection of animal and vegetal hemispheres. From this they can be put into an orthogonal form that allows them to be compared with schemes of 6-gon partitioning.

Attention is drawn to the offsets that are the pairs of three-radiate junctions made where cleavage lines of the current cycle contact lines of a previous cycle. The M offsets are where division lines in two sister cells meet the line in their mother-cell and the C offsets are where lines in two cells of some cousin-relationship meet a line of an earlier cycle. The M and C offsets are formed by an approximately orthogonal succession of division lines.

PHILOSOPHICAL TRANSACTIONS OF THE ROYAL SOCIETY B BIOLOGICAL SCIENCES

(*a*) *The significance of the offsets*

The offsets are of interest because we can associate the recognized types of cleavage patterns, spiral and bilateral, with the senses of certain offsets. The laeotropic spiral cleavage in *Nereis* can be linked with sinistral offsets at the second and third cleavage cycles. The bilateral cleavage in *Styela* and *Xenopus* can be linked with mirror-image symmetry in the senses of offsets, particularly of the M offsets at the third cleavage cycle. The senses of offsets affect the cleavage pattern because they determine the way blastomeres sit with respect to each other.

The offsets aid 6-gon partitioning. They make three-radiate rather than four-radiate junctions, so the average number of neighbours of a blastomere is close to six for a large number of blastomeres (see above). Also importantly, the offsets tend to reduce the variance of the number of neighbours about the mean value. This is because the two division lines at an offset raise the number of neighbours of two progeny by one. Two division lines if they form an offset cannot, for example, raise the neighbour-value of one adjoining cell by two, as two randomly placed division lines might. An offset is the pattern in the KS tetrad, which is one of the tetrads in a lattice that preserves 6-gons given some choices of placement of division lines. The other tetrad of this lattice, the L tetrad, is not a common feature of embryonic cleavage patterns.

The reduction in the variance of the number of neighbours is secondarily attributable to an orthogonal succession of cleavage lines because an M offset is always created at an orthogonal succession and cannot be created otherwise. An orthogonal succession may also equalize the numbers of neighbours of daughter cells if it divides the cell equally between opposite faces. An orthogonal succession of division lines was first noted last century in a number of tissues and is embodied in the various rules of Hofmeister, Sachs and Errera (see Korn & Spalding 1973).

Even so, variation in the numbers of neighbours of blastomeres at the completion of a cleavage cycle occurs in embryos (table 3). Whether it is less than the variation in numbers of neighbours around a typical polygon given a random choice of positions of cleavage lines is a complex mathematical problem not pursued here (but see a related problem in Cowan & Morris (1988)). We suggest simply that certain features of cleavage patterns, the offsets and the successive orthogonal divisions, may bias the random partitioning towards 6-gons.

Epithelial cells may in general divide in an orthogonal succession, creating M offsets. There are good examples of an orthogonal succession in plant tissues. Korn & Spalding (1973) drew division lines contacting the mother-cell wall in a study of the geometry of epidermal cell walls. More recently, an orthogonal succession has been formalized in the S and Z tetrads in plant meristematic epidermal cells by Lück *et al.* (1988). In animals, an orthogonal succession is observed in early embryonic cleavage cycles; and we have observed in *Xenopus* blastulae between the 64-cell and 256-cell stages successive division lines that were orthogonal and formed an M offset; the division lines formed either side of the midbody. But in animals at later stages of development and in renewal tissues, the pattern of successive division planes in proliferative epithelia is not generally known.

(*b*) *The role of cleavage patterns*

The remarkable aspects of cleavage are the conserved nature of cleavage patterns in some major divisions of the animal kingdom and their likeness to partitioning based on mechanical principles. This can be understood if cleavage patterns are stable forms of cytoplasmic partitioning.

PHILOSOPHICAL TRANSACTIONS OF THE ROYAL SOCIETY B BIOLOGICAL SCIENCES

Thompson (1917) wrote that cleavage patterns could be explained by mechanical forces. The partitions between cells behaved as fluid or semi-fluid films and followed Errera's rule that space is enclosed by a partition of minimal area. He showed the minimal area required to bisect an octant of a sphere is an anticlinal wall. Such a wall is between a radial wall of the octant and the outside of the sphere, and indeed the fourth cleavage lines we report as parallel to either a first or second line are examples of anticlinical walls. He showed patterns of soap bubbles created in a petri dish resembled cleavage forms.

Wilson (1925), on the other hand, believed cleavage patterns were more than a simple mechanical partitioning of the egg. He argued that cleavage patterns had a formative role in development and that blastomeres had promorphological values related to the adult form. We suggest that cleavage patterns divide the cytoplasm of the zygote in a mechanically stable way from the outset. Partitions form in positions that are stable when completed and are not rearranged later as in a soap bubble with fluid walls. Mechanical stresses in intercellular junctions are thus reduced and blastomeres do not move relative to one another after cleavage membranes have formed. In plants, it is accepted that division planes are correctly pre-positioned before being laid down because plants have rigid cell walls and so could not rearrange partitions later (Gunning 1982). But animal cells may not rearrange after a division either.

Evidence that intercellular junctions are stable during early cleavage is found in scanning electron micrographs of cleavage furrow formation in newt embryos (Ohshima & Kubota 1985). The cleavage furrow is a trough above the contractile ring. The sides of the furrow are wide at first, but later the sides are zipped together by interacting lamellipodia refastening regions of cytoplasm, covered now by plasma membranes, that had just been cleaved in two. Early cleavage divisions may partition the cytoplasm yet exclude rearrangement of previously contiguous regions. During later cleavage stages, spatial associations between cells are stabilized by specialized junctional complexes.

Spatial organization is built into the egg during oogenesis and is added to during ooplasmic segregation following sperm entry (Gerhart *et al.* 1984). The problem of cleavage can be seen as how to maintain this organization during the process of partitioning the zygote. A mechanically stable cleavage pattern could achieve this, though we do not rule out additional mechanisms to preserve spatial information in a developing embryo. Spatial stability may also be needed later during proliferation in many-celled epithelia where cell fates are emerging, and so there also the pattern should be biased towards cells with six neighbours. We suggest cleavage patterns and later cell-division patterns preserve the epigenetic progress made in preceding stages.

Thus we bring together the views of Thompson and Wilson and say that cleavage is both (*a*) subservient to mechanical principles and (*b*) supportive of the formative role of the cytoplasm in development.

(*c*) *How are cleavage patterns controlled?*

The partitioning of zygotic cytoplasm in a mechanically stable way is likely to involve the cytoskeleton. A cytoskeletal scaffold with attachments to the plasma membrane (Lazarides 1980; Schliwa & Blerkom 1981) may sense the shape of a cell and its junctions with neighbouring cells and so respond with a mechanically stable partition. Mechanical forces may be equalized along contiguous membranes by offsets of the same sense, as is observed along the first cleavage line in some embryos of *Xenopus*. In *Drosophila*, the cytoskeleton delineates cellular zones at the surface of the blastoderm before the cytoplasm is divided into cells by

plasma membranes (Warn & Warn 1986). But a stable partition pattern may also be pre-formed in the egg cytoplasm, which would explain the highly conserved patterns of cleavage.

(*d*) *Classical types of cleavage pattern*

In his monograph, Wilson (1925) noted three main geometrical forms of cleavage, radial (or orthoradial), spiral and bilateral. It is probably because of Wilson's writings that these three forms of cleavage are in the literature today. As examples of orthoradial cleavage he gave Selenka's now-famous drawings of cleavage in *Synapta* and Boveri's equally well-known drawings of *Paracentrotus* (*Strongylocentrotus*). The term orthoradial was introduced earlier by Conklin (1897) specifically to mean the form of cleavage in which there are two systems of cleavage planes, one meridional and radially symmetrical to the egg axis and another that intersects the meridians at right angles. But Conklin was certain that the orthoradial type was exceedingly rare and never found beyond the first few divisions. A polar or cross furrow, he wrote, was sufficient evidence that cleavage was not strictly orthoradial and he found such furrows usually present in the eggs of *Asterias* and *Arbacea* (Echinodermata). The most common representative of the radial type of cleavage, Conklin said, was the spiral form, not the orthoradial form. That he could class spiral cleavage as a form of radial cleavage was because of the radial symmetry of the spiral pattern. He thought Wilson's ranking of spiral cleavage as a type equal to radial was open to objection because it carried the suggestion that there was such a thing as spiral symmetry. To Conklin, there was only radial symmetry and bilateral symmetry and thus radial cleavage and bilateral cleavage. So, spiral cleavage with its radial symmetry was within the radial type. Wilson (1925) agreed to the extent that he saw the remarkable regularity of the spiral pattern viewed from one pole possessed a symmetry that was radial in type.

It would be confusing today to re-introduce the idea that spiral cleavage is a form of radial cleavage, but there is a need to consider the status of orthoradial cleavage. We regard orthoradial cleavage with its four-radiate junctions between cleavage lines and multi-radiate junctions at the poles, more a conceptual than an actual form that exists to any extent in embryos. Thompson (1917) himself questioned the existence of four-radiate junctions, noting their absence in the careful observations by Rauber of cleavage in amphibians.

If the orthoradial form is simply a stylized representation of cleavage, we are left with the spiral and bilateral types. Conklin (1897) limited the term 'spiral' to instances where cleavages are in the same direction in each quadrant. The term direction here means the positioning of blastomeres to the left or right of those more vegetally placed. Where the direction is changed in one or more quadrants, cleavage is termed oblique. If it is changed in two quadrants symmetrically, the cleavage is bilateral as well. Thus bilateral cleavage is derivable from spiral cleavage by a change in the direction of cleavage in two quadrants. In the present topological analysis, we have seen that the direction of cleavage, that is how blastomeres sit with respect to those vegetally placed, depends on the senses of the offsets and so types of cleavage can be defined to some extent by the senses of offsets, in the way the all-sinistral offsets at the third cleavage cycle in *Nereis* define the spiral type and the mirror-image M offsets of the third cleavage cycle in *Styela* and *Xenopus* define the bilateral type.

The work was supported by the Australian Research Grants Scheme. We thank June Jeffery who drew the figures.

PHILOSOPHICAL TRANSACTIONS OF THE ROYAL SOCIETY B BIOLOGICAL SCIENCES

References

Abbott, L. A. & Lindenmayer, A. 1981 Models for growth of clones in hexagonal cell arrangements: applications in *Drosophila* wing disc epithelia and plant epidermal tissues. *J. theor. Biol.* **90**, 495–514.

Berrill, N. J. & Karp, G. 1976 *Development*. New York: McGraw-Hill.

Cleine, J. H. & Dixon, K. E. 1985 The effect of egg rotation on the differentiation of primordial germ cells in *Xenopus laevis*. *J. Embryol. exp. Morph.* **90**, 79–99.

Conklin, E. G. 1897 The embryology of *Crepidula*, a contribution to the cell lineage and early development of some marine gasteropods. *J. Morph.* **13**, 1–226.

Conklin, E. G. 1905 The organization and cell-lineage of the ascidian egg. *J. Acad. nat. Sci. Philad.* (2nd ser.) **13**, 1–119.

Cowan, R. 1978 The use of the ergodic theorems in random geometry. *Adv. appl. Probab.* **10** (Suppl.), 47–57.

Cowan, R. & Morris, V. B. 1988 Division rules for polygonal cells. *J. theor. Biol.* **131**, 33–42.

Dale, L. & Slack, J. M. W. 1987 Fate map for the 32-cell stage of *Xenopus laevis*. *Development* **99**, 527–551.

Gerhart, J. C., Vincent, J.-P., Scharf, S. R., Black, S. D., Gimlich, R. L. & Danilchik, M. 1984 Localization and induction in early development of *Xenopus*. *Phil. Trans. R. Soc. Lond.* B **307**, 319–330.

Gunning, B. E. S. 1982 The cytokinetic apparatus: its development and spatial regulation. In *The cytoskeleton in plant growth and development* (ed. C. W. Lloyd), pp. 229–292. London: Academic Press.

Hirose, G. & Jacobson, M. 1979 Clonal organization of the central nervous system of the frog. I. Clones stemming from individual blastomeres of the 16-cell and earlier stages. *Devl Biol.* **71**, 191–202.

Kirschner, M. W. & Hara, K. 1980 A new method for local vital staining of amphibian embryos using Ficoll and "crystals" of Nile Red. *Mikroskopie* **36**, 12–15.

Korn, R. W. & Spalding, R. M. 1973 The geometry of plant epidermal cells. *New Phytol.* **72**, 1357–1365.

Lazarides, E. 1980 Intermediate filaments as mechanical integrators of cellular space. *Nature, Lond.* **283**, 249–256.

Lewis, F. T. 1926 The effect of cell division on the shape and size of hexagonal cells. *Anat. Rec.* **33**, 331–355.

Lewis, F. T. 1943 The geometry of growth and cell division in epithelial mosaics. *Am. J. Bot.* **30**, 766–776.

Lindenmayer, A. 1984 Models for plant tissue development with cell division orientation regulated by preprophase bands of microtubules. *Differentiation* **26**, 1–10.

Lück, J., Lindenmayer, A. & Lück, H. B. 1988 Models of cell tetrads and clones in meristematic cell layers. *Bot. Gaz.* **149**, 127–141.

Moody, S. A. 1987 Fates of the blastomeres of the 16-cell stage *Xenopus* embryo. *Devl Biol.* **119**, 560–578.

Nakamura, O. & Kishiyama, K. 1971 Prospective fates of blastomeres at the 32 cell stage of *Xenopus laevis* embryos. *Proc. Japan Acad.* **47**, 407–412.

Nieuwkoop, P. D. & Faber, J. 1956 Normal table of *Xenopus laevis* (Daudin). Amsterdam: North-Holland.

Ohshima, H. & Kubota, T. 1985 Cell surface changes during cleavage of newt eggs: scanning electron microscopic studies. *J. Embryol. exp. Morph.* **85**, 21–31.

Schliwa, M. & van Blerkom, J. 1981 Structural interaction of cytoskeletal components. *J. Cell Biol.* **90**, 222–235.

Thompson, D'A. W. 1917 *On growth and form*. Cambridge: University Press.

Warn, R. M. & Warn, A. 1986 Microtubule arrays present during the syncytial and cellular blastoderm stages of the early *Drosophila* embryo. *Expl Cell Res.* **163**, 201–210.

Wilson, E. B. 1892 The cell-lineage of *Nereis*. *J. Morph.* **6**, 361–480.

Wilson, E. B. 1925 *The cell in development and heredity*. New York: Macmillan.

Appendix. Symbols and conventions used in all figures

I	first cleavage line
II	second cleavage line
III	third cleavage line
IV	fourth cleavage line
V	fifth cleavage line
VI	sixth cleavage line
dex	dextral offset
heavy continuous line	first cleavage line
heavy dashed line	second cleavage line
LD	left dorsal quadrant of *Xenopus*
LV	left ventral quadrant of *Xenopus*
RD	right dorsal quadrant of *Xenopus*
RV	right ventral quadrant of *Xenopus*
sin	sinistral offset

PHILOSOPHICAL TRANSACTIONS OF THE ROYAL SOCIETY B BIOLOGICAL SCIENCES